NASA/TM—2012–217476

Compact Fuel Element Environment Test

D.E. Bradley
Yetispace, Inc., Huntsville, Alabama

O.R. Mireles, R.R. Hickman, and J.W. Broadway
Marshall Space Flight Center, Huntsville, Alabama

December 2012

The NASA STI Program…in Profile

Since its founding, NASA has been dedicated to the advancement of aeronautics and space science. The NASA Scientific and Technical Information (STI) Program Office plays a key part in helping NASA maintain this important role.

The NASA STI Program Office is operated by Langley Research Center, the lead center for NASA's scientific and technical information. The NASA STI Program Office provides access to the NASA STI Database, the largest collection of aeronautical and space science STI in the world. The Program Office is also NASA's institutional mechanism for disseminating the results of its research and development activities. These results are published by NASA in the NASA STI Report Series, which includes the following report types:

- TECHNICAL PUBLICATION. Reports of completed research or a major significant phase of research that present the results of NASA programs and include extensive data or theoretical analysis. Includes compilations of significant scientific and technical data and information deemed to be of continuing reference value. NASA's counterpart of peer-reviewed formal professional papers but has less stringent limitations on manuscript length and extent of graphic presentations.

- TECHNICAL MEMORANDUM. Scientific and technical findings that are preliminary or of specialized interest, e.g., quick release reports, working papers, and bibliographies that contain minimal annotation. Does not contain extensive analysis.

- CONTRACTOR REPORT. Scientific and technical findings by NASA-sponsored contractors and grantees.

- CONFERENCE PUBLICATION. Collected papers from scientific and technical conferences, symposia, seminars, or other meetings sponsored or cosponsored by NASA.

- SPECIAL PUBLICATION. Scientific, technical, or historical information from NASA programs, projects, and mission, often concerned with subjects having substantial public interest.

- TECHNICAL TRANSLATION. English-language translations of foreign scientific and technical material pertinent to NASA's mission.

Specialized services that complement the STI Program Office's diverse offerings include creating custom thesauri, building customized databases, organizing and publishing research results…even providing videos.

For more information about the NASA STI Program Office, see the following:

- Access the NASA STI program home page at <http://www.sti.nasa.gov>

- E-mail your question via the Internet to <help@sti.nasa.gov>

- Fax your question to the NASA STI Help Desk at 443–757–5803

- Phone the NASA STI Help Desk at 443–757–5802

- Write to:
  NASA STI Help Desk
  NASA Center for AeroSpace Information
  7115 Standard Drive
  Hanover, MD 21076–1320

NASA/TM—2012–217476

Compact Fuel Element Environment Test

D.E. Bradley
Yetispace, Inc., Huntsville, Alabama

O.R. Mireles, R.R. Hickman, and J.W. Broadway
Marshall Space Flight Center, Huntsville, Alabama

National Aeronautics and
Space Administration

Marshall Space Flight Center • Huntsville, Alabama 35812

December 2012

Acknowledgments

This work was done with the support of NASA Marshall Space Flight Center's ER24, Propulsion Research and Development Branch, and EM32, Metal Joining & Processes Branch, as part of the Nuclear Cryogenic Propulsion Stage project under NASA's Advanced Exploration Systems program. Thank you to Jim Martin, Bill Emrich, Jeramie Broadway, John Bossard, Keith Chavers, Mark Black, and Tabitha Smith for their significant contribution to the design, construction, and testing of the compact fuel element environment test.

TRADEMARKS

Available from:

NASA Center for AeroSpace Information
7115 Standard Drive
Hanover, MD 21076–1320
443–757–5802

This report is also available in electronic form at
<https://www2.sti.nasa.gov/login/wt/>

TABLE OF CONTENTS

TABLE OF CONTENTS (Continued)

LIST OF FIGURES

LIST OF FIGURES (Continued)

LIST OF TABLES

LIST OF ACRONYMS, SYMBOLS, AND ABBREVIATIONS

BN	boran nitride
cermet	ceramic metal composite
CFEET	compact fuel element environment test
DAQ	data acquisition
h-BN	hexagonal boron nitride
IR	infrared
I_{sp}	specific impulse
JHA	job hazard analysis
NTP	nuclear thermal propulsion
NTR	nuclear thermal rocket
RF	radio frequency
SLPM	standard liters per minute
W-Re-HfN	tungsten-rhenium-hafnium nitride

TECHNICAL MEMORANDUM

COMPACT FUEL ELEMENT ENVIRONMENT TEST

1. INTRODUCTION

The mechanical failure of fuel elements exposed to hydrogen at very high temperatures is a high-risk liability to the successful implementation of nuclear thermal rockets (NTRs). The fissile nuclear material used in such fuel elements to generate very high heating density requires a stable support matrix that is robust enough to persist in the presence of flowing hydrogen at reactor temperatures up to 2,727 °C (3,000 K). Thus, the testing of candidate support materials without the inclusion of fissile nuclear materials is proposed to reduce the great expense of nuclear infrastructure during early testing. Such a study will leverage existing research to narrow the field of likely material candidates and then exercise frequent test iterations to focus on the best materials and manufacturing practices. With this knowledge, fuel elements may then be fabricated to include fissile material for prototypical testing in a reactor environment. Without the thermal energy generated by the nuclear fuel, an alternative for noncontact volumetric heating of fuel elements during testing is required. Radio frequency (RF) heating fulfills both of these requirements and is proposed for low-cost testing of candidate materials.

2. BACKGROUND

Deep space missions with large payloads require high specific impulse (I_{sp}) and relatively high thrust to achieve mission goals in reasonable timeframes.[1] Conventional, storable propellants produce average I_{sp}. NTRs capable of high I_{sp} thrust have been proposed. An NTR employs heat produced by fission reaction to heat and therefore accelerate hydrogen, which is then forced through a rocket nozzle providing thrust. Fuel element temperatures are very high (up to 2,727 °C (3,000 K)) and hydrogen is highly reactive with most materials at high temperatures. Data covering the effects of high-temperature hydrogen exposure on fuel elements are limited. The primary concern is the mechanical failure of fuel elements, which employ high melting point metals, ceramics, or a combination (cermet) as a structural matrix through which fissile material is distributed. It is not necessary to include fissile material in test samples intended to explore high-temperature hydrogen exposure of the structural support matrices. The small-scale test bed known as compact fuel element environment test (CFEET) was designed to heat fuel element samples via noncontact RF heating and expose samples to hydrogen to assist in optimal material and manufacturing process selection without employing fissile material. This Technical Memorandum details the test bed design and development, and the results of testing conducted to date.

3. TEST SETUP

3.1 Hardware Description

Existing hardware was available to set up an RF heating system. Because of this convenience, and the overall system similarity to an existing larger scale NTR environmental simulator, the nuclear thermal rocket element environmental simulator, an RF heating system operating on the fuel elements in a vacuum chamber, was assembled.[2] The use of subscale hardware added the benefit of rapid turnaround studies of component changes such as coil configurations and fuel sample insulators. Finally, hardware operational experience was readily obtained with a small-scale system due to very low operating expense. This experience provided the necessary background experience to assess and evaluate RF heating system designs and to understand noncontact temperature measurement via pyrometry.

The test hardware used a very small custom-fabricated chamber, shown in figure 1, that had a diameter of 10 in and a height of 18 in, and was capable of vacuum levels to 10×10^{-6} T. The chamber was integrated with a 15-kW RF power supply via a vacuum-rated RF power feedthrough.

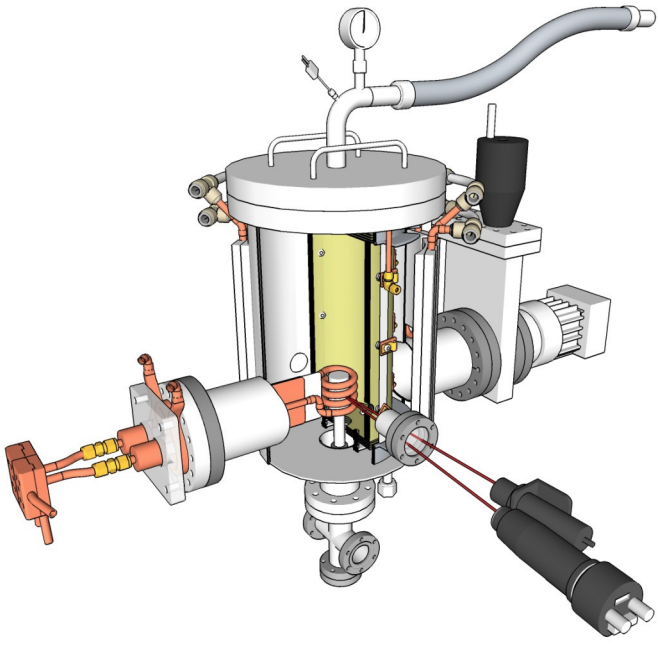

Figure 1. CFEET computer-aided design model with chamber cutaway showing RF coil.

The RF heating coil was located inside the chamber and was fabricated from copper tubing. The copper tubing functioned both as a water-cooling channel and as the electrical current conductor. The chamber was provided to contain any potential fuel element reactants and to limit heat loss from the fuel element during test.

The chamber was equipped with a full-diameter top flange to allow access to larger in-chamber subassemblies, such as the RF coil, the fuel element support pedestal, and the thermal radiation shields (if equipped). Three 2.75-in Conflat® flange ports provided chamber venting, in-chamber instrumentation, and an optical viewport for noncontact pyrometric measurement of the fuel element temperature. Two 6-in Conflat flange ports interfaced with the RF power feedthrough and a vacuum turbopump via a gate valve. Finally, a 4-in Conflat flange at the base of the chamber allowed fuel elements to be rapidly installed/removed once final configuration arrangements of larger internal components were properly positioned from above.

3.2 Pyrometry

The temperature of a prototypical NTR fuel element during operation is as high as 2,727 °C (3,000 K). Because of the very high desired temperatures of operation, physical contact with the surrogate fuel element is not practical. To measure these temperatures, pyrometry was employed. Pyrometers measure light intensity in one or more wavelengths, assume an emissivity, and thereby produce a temperature reading per the Stefan-Boltzmann law for gray bodies:

$$j^* = \varepsilon\sigma T^4 \,, \tag{1}$$

where

j^* = irradiance or emissive power (J/s·m^2)
ε = surface emissivity (blackbody =1, graybody <1)
σ = Stefan-Boltzmann constant = 5.6704×10^{-8} J/s·m^2·K^4
T = surface temperature (K).

An example of a pyrometer is a small handheld infrared (IR) temperature measurement device (shown in fig. 2) commonly equipped with a laser aiming spot often used for the troubleshooting of HVAC equipment or for detecting hot spots in cooling systems. These pyrometers make an assumption regarding the surface emissivity of the measured component. Emissivity, however, varies both with temperature (and more dramatically at high temperature) and wavelength, and cannot be assumed to be constant, as evidenced in figure 3.

Figure 2. Example of handheld IR pyrometer.

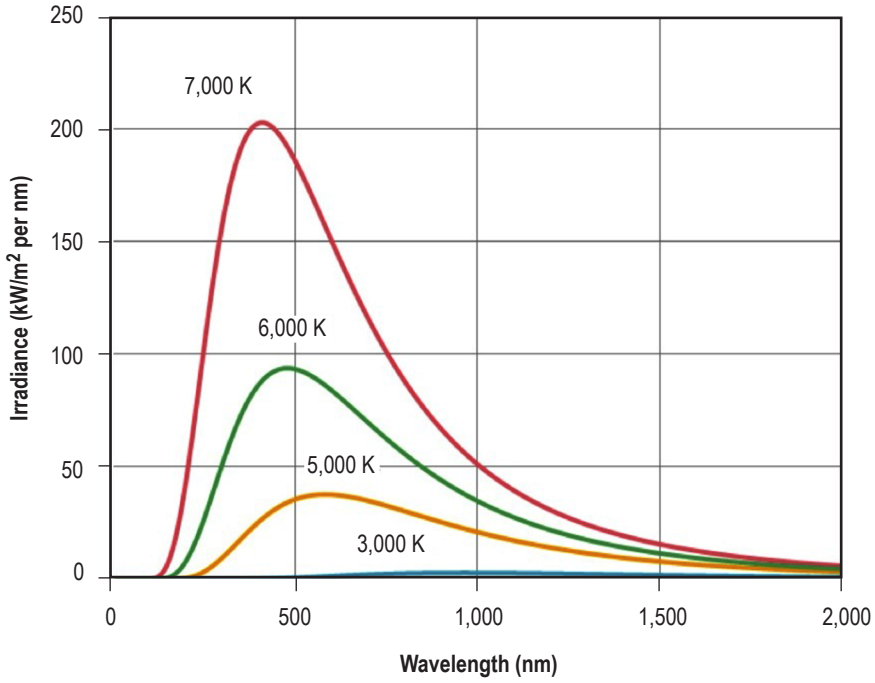

Figure 3. Planck's law irradiance versus wavelength versus temperature.

By measuring intensity at several discrete wavelengths and relying on Planck's law, which relates electromagnetic energy to wavelength radiated by blackbodies, emissivity can be determined real time and therefore used to provide a reliable temperature reading.[3] Both a FAR™ multiwavelength pyrometer and a Mikron™ M770S two-color pyrometer were used for fuel element temperature measurement.

3.3 Data Acquisition System

During the process of developing system hardware, the complexity of the data acquisition (DAQ) system evolved. A total of three different DAQ configurations were used at different stages of testing.

In general, operational parameters of the RF power supply and resulting sample element temperatures were of primary interest. Later in development, water-cooled system components were instrumented to make reasonably accurate estimates of heating rates. The DAQ system progressed from a single four-channel USB card to an Agilent™ 34972A multiplexer with 10 thermocouple channels and 10 ± 10 VDC channels. Table 1 describes the recorded channels.

Table 1. DAQ channels.

Channel ID	Channel Description	Measurement Range	Signal Type
101 flex in	Cooling water temperature entering RF power supply	–200 to 1,350 °C	Type K TC
102 flex out	Cooling water temperature exiting RF power supply	–200 to 1,350 °C	Type K TC
103 coil in	RF coil cooling water temperature inlet	–200 to 1,350 °C	Type K TC
104 coil out	RF coil cooling water temperature outlet	–200 to 1,350 °C	Type K TC
105 gas in	Flowing gas inlet temperature	–200 to 1,350 °C	Type K TC
106 gas out	Flowing gas outlet temperature	–200 to 1,350 °C	Type K TC
107 flange in	RF flange cooling water inlet temperature	–200 to 1,350 °C	Type K TC
108 flange out	RF flange cooling water outlet temperature	–200 to 1,350 °C	Type K TC
109 jacket in	CFEET chamber water jacket water inlet temperature	–200 to 1,350 °C	Type K TC
110 jacket out	CFEET chamber water jacket water outlet temperature	–200 to 1,350 °C	Type K TC
111 Mikron temperature	Mikron M770S pyrometer temperature	600 to 1,400 °C	4 to 20 mA
112 FAR temperature	FAR pyrometer temperature	800 to 2,500 °C / 2,000 to 4,000 °C	±10 VDC
113 FAR emissivity	FAR pyrometer surface emissivity	0 to 1	±10 VDC
114 vacuum UHV	Hot filament ion gauge	10^{-3} to 10^{-10} torr	±10 VDC
115 vacuum 1 torr	Diaphragm gauge	760 to 10^{-3} torr	±10 VDC
116 RF power	Flexitune RF power output	0 to 15 kW	0 to 4 VDC
117*	N/A	N/A	N/A
118 RF frequency	Flexitune RF power output frequency	20 to 60 kHz	0 to 4 VDC
119 RF voltage	Flexitune RF power output voltage	0 to 150 V rms	0 to 4 VDC
120 RF current	Flexitune RF power output current	0 to 2,400 A rms	0 to 4 VDC

* Open circuit in wiring harness conductors.

In addition to these data channels, the FAR pyrometer was equipped with its own data logging capability including temperature, tolerance, and emissivity, based on recording the full spectrum of incident light intensity data between wavelengths of 500 to 1,000 nm. A wiring schematic for this instrumentation is provided in appendix A.

3.4 Cooling Water System

The purpose of this experiment was to generate a tremendous amount of heat in a relatively small fuel element sample. In an NTR, this heat would be transferred to a propellant, which would then be used in a rocket nozzle to generate thrust. In the case of this test hardware, all generated heat energy must be managed for safety and control.

The RF power system employed water-cooled copper conductors to maintain constant material resistivity and to extract all excess heat generated due to the very large currents and relatively small conductor cross-sectional areas. The water cooling of the RF power supply conductors must have a carefully monitored conductivity to prevent erosion of brazed/soldered components. Completely mineral-free water would attack braze and solder materials, whereas too high a conductivity due to dissolved solids would provide stray current pathways within the water versus the copper conductors. As a result, the overall water cooling system consisted of two separate subsystems: (1) A Polyscience™ water-to-water recirculating cooler used to cool the RF power supply (as shown in figs. 4 and 5) and (2) a 14,000 W Dimplex™ refrigerated chiller used for general water cooling that was located outside the lab space and supplied chilled water via easily reconfigured manifolds (see fig. 6). The complete water cooling system schematic is shown in appendix B.

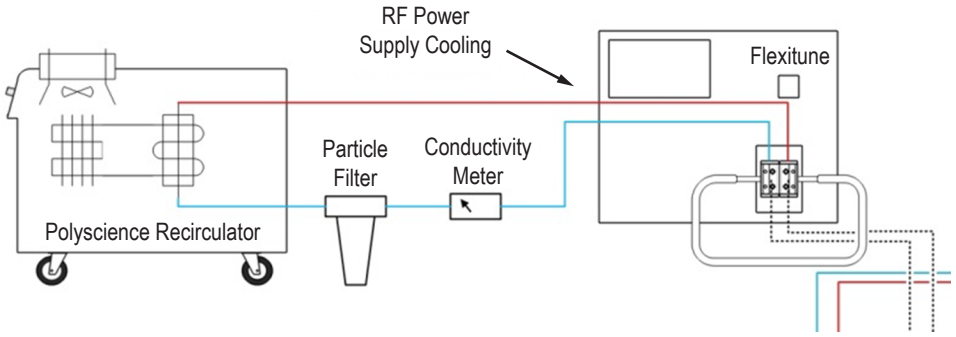

Figure 4. Conductivity-monitored RF power supply water-cooling schematic.

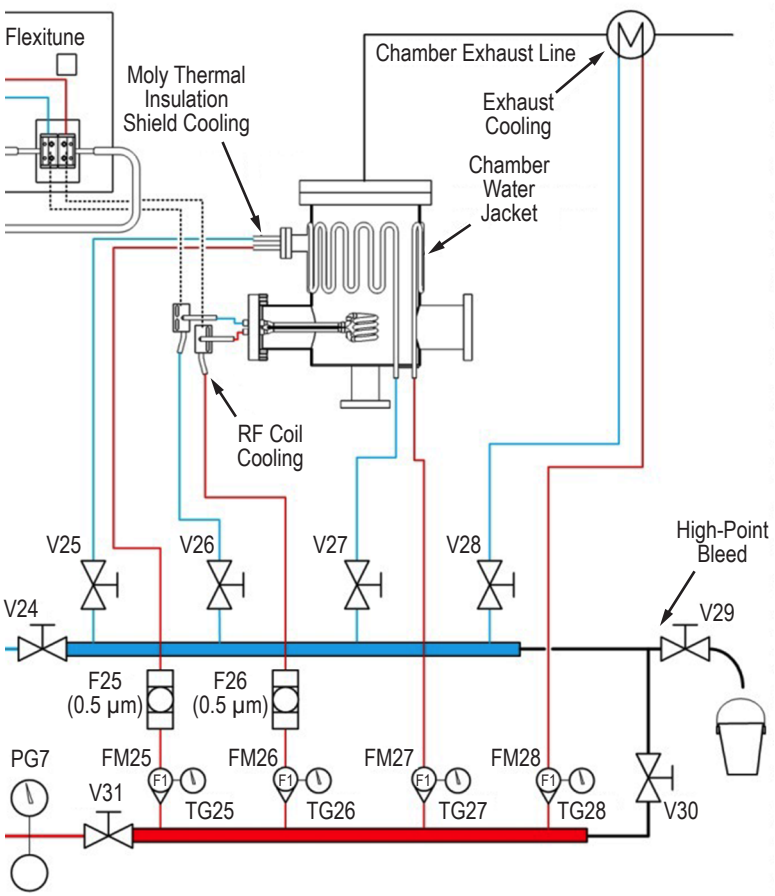

Figure 5. High-capacity water-cooling locations and manifold.

Figure 6. General purpose water-cooling manifolds.

3.5 Hydrogen Gas Flow System

The exposure of a heated sample to flowing hydrogen gas is required to adequately assess the ability of the sample to survive a typical NTR environment. A low-flow-rate hydrogen gas system was integrated with the testing hardware and included a purge system using Argon gas and a vacuum scroll pump along with sufficient control and isolation valves and a mass flow controller as shown in figure 7.

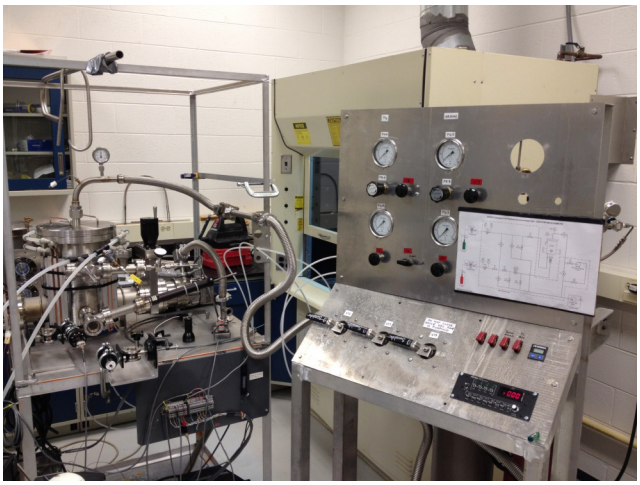

Figure 7. Gas control system.

During testing, the sample was subjected to predetermined conditions of temperature, hydrogen flow rate, and duration simulating exposure during a typical mission thrust profile. A detailed schematic of the gas control system is provided in appendix C, and a component descriptor for the gas system schematic is given in appendix D.

The exhaust of the system was directed out through a hydrogen burn stack to a fume hood, and the lab space was equipped with a room oxygen detector. Portable oxygen detectors and hydrogen detectors ensured personnel safety during testing.

4. MODELING AND ANALYSIS

4.1 Thermal Cycling of Tungsten-Rhenium-Hafnium Nitride Surrogate Sample Element

A small, 1/2-in-diameter, 308 stainless steel rod was used for initial checkout testing of the apparatus, as it is nonmagnetic and emissivity for steel at temperature is well known. Its melting point of ≈1,500 °C, however, limited the ability to test the hardware to levels required for nuclear thermal propulsion (NTP) fuel element evaluation.

One-half-inch-diameter tungsten-rhenium-hafnium nitride (W-Re-HfN) cermet slugs were provided for high-temperature testing. The estimated mass composition and properties are provided in table 2.[4]

Table 2. W-Re-HfN sample properties.

Component	Mass (%)	Specific Heat, *Cp* (J/Kg·K)	Melting Point (°C)
W	63	132	3,422
Rh	5	136	3,186
HfN	32	249	3,305
Final properties per mass (%)		161.6	3,378.5

Two elements were provided for testing, both with a diameter of 1/2-in. The first element was 1.5 in long and ≈93 g; the second element was 2 in long and 124 g. Both elements were tested to failure, as shown in figure 8, which occurred when the elements were heated to a recorded temperature of 2,565 °C (2,838 K).

Figure 8. W-Re-HfN samples, before testing and after failure.

4.2 Paschen Curve—Electrical Arcing of Radio Frequency Coil

Electrical arcing may take place between conductors with a net voltage difference between them due to ionization of their separating atmosphere. The voltage at which this arcing takes place depends on the pressure of the atmosphere and the proximity between the conductors.

With a fixed proximity between the conductors in a given atmosphere, the voltage at which arcing will occur is very high at low pressures, drops to a minimum voltage at an intermediate pressure, and then increases with increasing gas pressure. This relationship is characterized by the Paschen curve for a particular atmosphere, as shown in figure 9.[5]

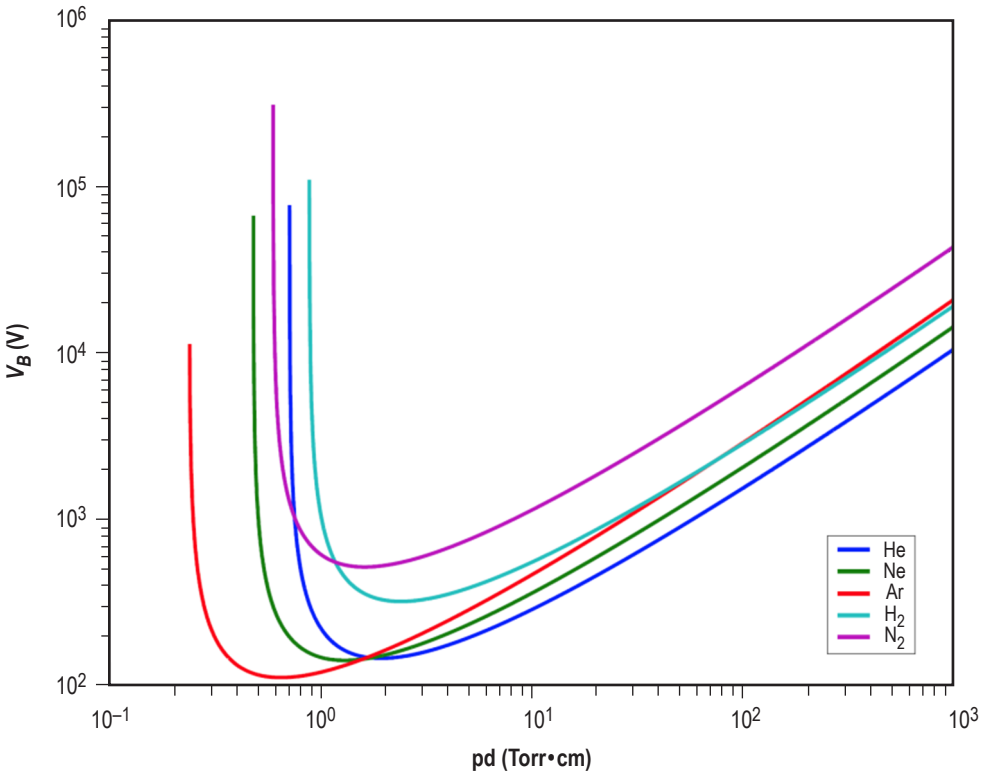

Figure 9. Paschen curve for various gases.

Take the particular Paschen curve for hydrogen gas in figure 10. Assuming the conductors in question are 1 cm apart, there is a direct relationship between the arcing voltage threshold and the hydrogen gas pressure. This means that the arcing voltage threshold is ≈584 V for a hydrogen gas pressure of 10 Torr (0.2 psi).

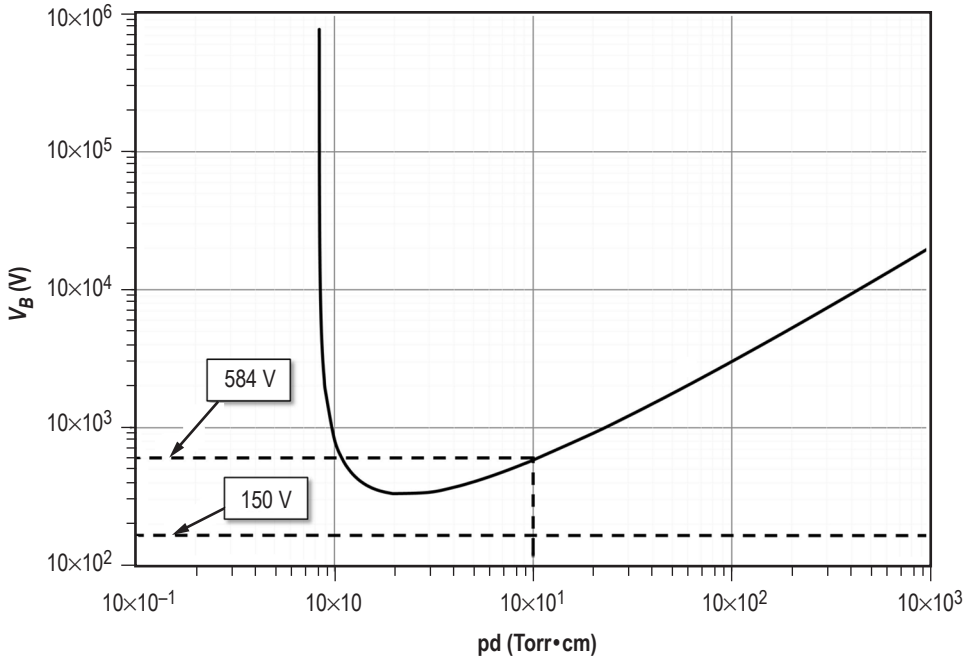

Figure 10. Paschen curve for hydrogen gas showing arcing threshold (584 V) at 10 Torr·cm.

Thus, if an RF coil operates in a hydrogen gas atmosphere of 10 T, and the distance between two turns of the coil is 1 cm, ionization of the hydrogen gas leading to arcing would occur at an applied voltage of 584 V and above. Below that, arcing would not occur. In the case of the RF power supply used in this testing, the maximum applied voltage was 150 V. Arcing should therefore not be possible at any time when operating in a hydrogen atmosphere. In contrast, the Paschen curves for helium, neon, and argon present far less resistance to arcing, whereas nitrogen has an even higher resistance to arcing than hydrogen.

For testing, arcing was precluded by performing a basic analysis of conductor-to-conductor proximity, atmospheric content, and applied voltage.

4.3 Thermodynamic Model

The sample element to be heated was simply supported vertically by a hollow pedestal made of hexigonal boron nitride (h-BN), a ceramic with a melting (sublimation) point of 2,973 °C (3,246 K). An h-BN cylindrical insulator was installed around the sample but within the RF coil in such a way as to prevent direct contact with the sample and with the coil. It was also simply supported by the pedestal and acted as a flow channel for any gas that was applied to the sample via the hollow pedestal. A small hole was provided in the side of the insulator to allow temperature measurement via optical pyrometer between turns of the RF coil. This setup is shown in figure 11.

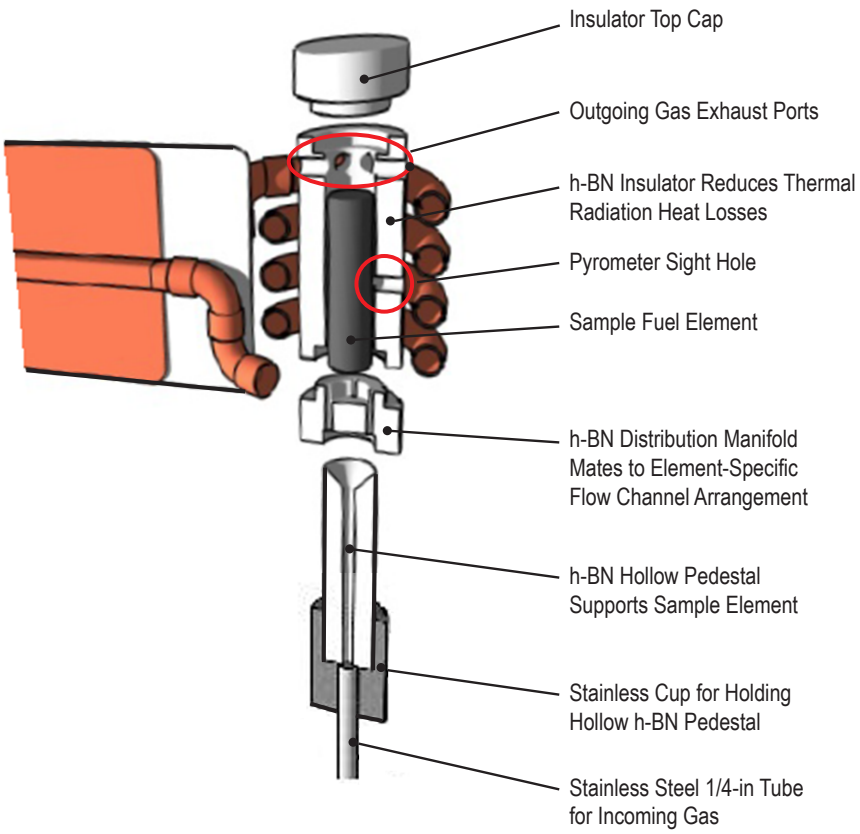

Figure 11. Sample element support and insulator details.

Thermal energy was supplied to the fuel element via RF heating and was lost by thermal radiation, thermal conduction, and convection. In the case of vacuum operations, loss was strictly via radiation and conduction. The thermal conduction loss took place at the interface between the fuel sample and the support pedestal, and to a lesser extent, with the surrounding atmosphere during nonvacuum operations. The fuel sample lost heat via thermal radiation to the inside of the insulator and had a limited line of sight to the chamber optical pyrometer port. The insulator, in turn, radiated to both the RF coil and the vacuum chamber wall in ratios defined by the geometry of the insulator and the RF coil. The emissivity of the fuel sample and the insulator changed as they experienced a wide range of temperatures, whereas the emissivity of both the RF coil (copper) and the vacuum chamber wall (stainless steel) were relatively constant due to their more or less isothermal conditions provided by water cooling.

4.3.1 Relative Contribution of Radiation, Conduction, and Convection Heat Transfer

4.3.1.1 Thermal Radiation Heat Loss. Equation (2) displays the thermal radiation heat loss:

$$\dot{Q}_r = \varepsilon A_1 \sigma \left(T_1^4 - T_2^4 \right) , \tag{2}$$

where

$\dot{Q}_r$ = thermal radiation heat loss rate (W)
ε = surface emissivity (ideal blackbody = 1, graybody <1)
A_1 = surface area of radiating surface (m^2)
σ = Stefan-Boltzmann constant = 5.6704×10^{-8} J/s·m^2·K^4
T_1 = radiating body surface temperature (K)
T_2 = receiving body surface temperature (K).

4.3.1.2 Thermal Conduction Heat Loss. Equation (3) displays the thermal conduction heat loss:

$$\dot{Q}_c = kA\pi \frac{T_1 - T_2}{d} , \tag{3}$$

where

$\dot{Q}_c$ = thermal conduction heat loss rate (W)
k = thermal conductivity of h-BN insulator (W/m·K)
A = cross-sectional area of h-BN insulator (m^2)
T_1 = hot end temperature of h-BN insulator (heated sample element temperature) (K)
T_2 = cool end temperature of h-BN insulator (K)
d = length of boron nitride (BN) insulator (m).

4.3.1.3 Convection Heat Loss. Convection is heat loss between a solid surface and a moving fluid and is highly dependent on fluid properties and flow conditions. In general, low-density fluids (gases) at low flow velocities generate very low heat transfer rates. The effective heat transfer rate from the fuel element samples tested in CFEET was expected to be a small fraction of overall losses due to extremely low flow rates of very low density hydrogen gas. It was consequently omitted from the overall estimation of heating required to achieve sample temperature.

The results of these modes of heat loss are plotted together in figure 12 to provide steady state heat loss rates versus fuel element temperatures.

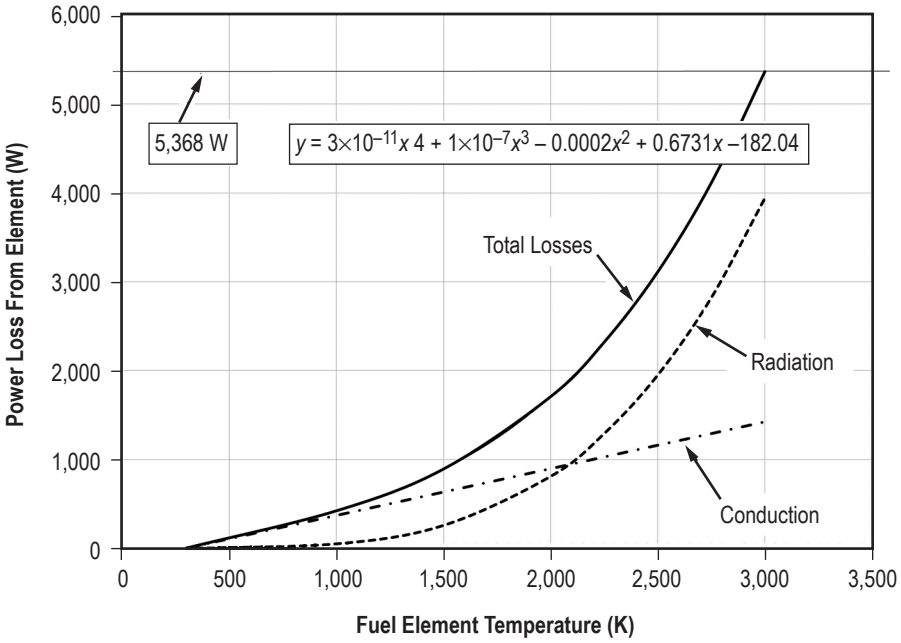

Figure 12. Thermodynamic model of sample element thermal losses versus temperature.

It stands to reason that, for a given steady state temperature, the effective RF heating rate equals the loss rate. The model therefore gave some estimate of RF heating efficiency when combined with the measured element temperature and the reported power supply output.

Conduction losses dominated up to around 1,800 °C (2,050 K), at which point thermal radiation losses dominated. According to the thermodynamic model, a net heat input to the sample of 5,368 W was required to achieve a sample temperature of 2,727 °C (3,000 K).

4.4 Radio Frequency Modeling

4.4.1 Radio Frequency Heating Coil, Operational Frequency, and Field Strength Modeling

The RF heating coil was a high-power inductor that generated a highly concentrated, alternating magnetic field centered along the inside of its axial length, as shown in figure 13.

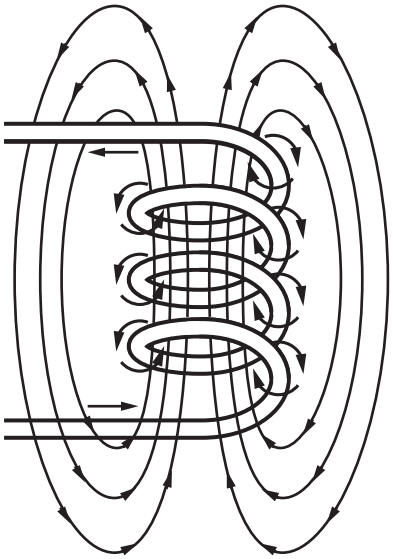

Figure 13. Radio frequency coil magnetic field (note concentration of field lines in center of coil).

The RF power supply used for this testing had an operational frequency range of 20 to 60 kHz. At the beginning of development, coils were simply hand bent, fitted, and tested to determine system operational frequency empirically, with tuning capacitors added or removed as required to shift operating frequency or improve total available output power. A schematic of the RF power system can be found in appendix E.

The need for better RF coupling efficiency to achieve higher sample temperatures drove the need for a tool to predict operating frequency based on coil geometry. A spreadsheet-based calculating model combined the various governing equations. Using the model, different geometries were rapidly screened to achieve an optimal configuration of coil resistance, inductance, and resonant frequency so that optimal designs could be selected and fabricated with some confidence in their ultimate operational parameters.

For the purposes of estimating operational frequency, the coil was considered to be a simple inductor with inductance L_{coil}:

$$L_{\text{coil}} = \frac{\mu_0 k_L N^2 A}{l} \ , \tag{4}$$

where

L_{coil} = coil inductance (H)
μ_0 = permeability of free space = $4\pi \times 10^{-7}$ H/m
k_L = Nagaoka coefficient = $[1 + 0.45(D/l)]^{-1}$
N = number of coil turns
A = area of cross section of the coil (m^2)
l = length of coil (m).

In figure 14, L_{coil} represents the heating coil and two instances of $L_{coil\ leg}$ represent the supply and return conductors to the coil, all of which were located outside of the RF power supply. The isolation transformer and tuning capacitors were located inside the RF power supply.

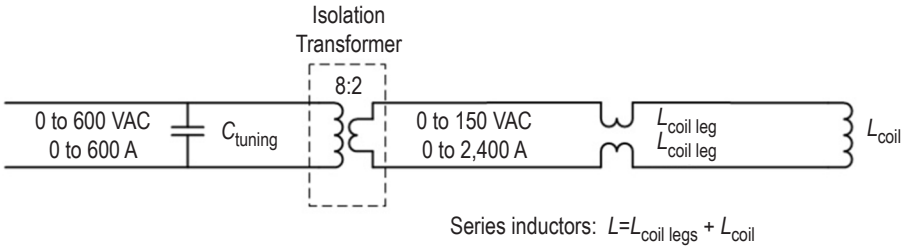

Figure 14. Radio frequency power supply output coil schematic.

The network was then simplified to an equivalent circuit yielding a single capacitance and a single inductance combined in parallel, as shown in figure 15.

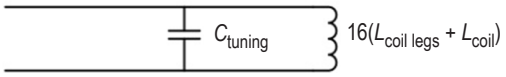

Figure 15. Radio frequency power supply output equivalent circuit.

The overall resistance of the conductors played a role in how much damping could be expected in the resonant resistance inductor capacitor network circuit formed by the conductors, capacitors, and the total inductance of the circuit. The resonant frequency or resulting RF operating frequency of the system is given by:

$$f(\text{Hz}) = \frac{1}{2\pi\sqrt{L_{total}C_{total}}}\ , \tag{5}$$

where

f = resonant frequency of LC network (Hz)
L_{total} = total system inductance (H)
C_{total} = total system capacitance (F).

The contribution of the legs to the overall inductance was reduced (and power available to heat sample at the coil, thereby maximized) by using a characteristic configuration known as a ‘fish tail,’ consisting of parallel flat conductor plates located as close as possible to each other, separated by an electrically insulating barrier, as shown in figure 16.

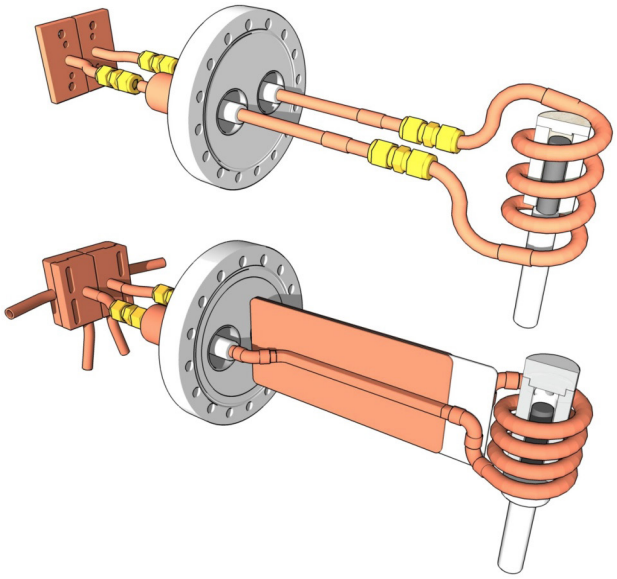

Figure 16. Radio frequency feedthrough configurations:
(a) With no fishtails and (b) with fishtails.

The geometric configuration of the coil populated the spreadsheet-based model producing an expected operational frequency, as shown in table 3.

Table 3. Results of operating frequency spreadsheet model.

Geometric Property	Coil A	Coil B	Coil C	Coil D	Coil E
D, diameter of coil (in)	2	1.25	1.875	1.875	2
N, number of turns	5	4	4	4	4
l, length of coil (in)	4	2.8	3	1.75	1.97
D, copper tube diameter (in)	0.25	0.25	0.375	0.375	0.5
C_{total}, total system capacitance (F)	3.3×10^{-6}	3.3×10^{-6}	3.3×10^{-6}	3.3×10^{-6}	3.3×10^{-6}
L_{coil}, coil inductance (H)	5.12×10^{-7}	1.86×10^{-7}	3.67×10^{-7}	5.44×10^{-7}	5.59×10^{-7}
L_{total}, total system inductance (H)	1.49×10^{-5}	0.97×10^{-5}	1.16×10^{-5}	0.88×10^{-5}	0.9×10^{-6}
f, system natural frequency (kHz)	22.7	28.1	25.7	29.5	29.1

In addition to determining operational frequency, the geometry was also used to calculate estimated resistance to current flow due to skin effect and mutual inductance of adjacent coil turns.

4.4.2 Radio Frequency Coil Resistance Heating of Coil Material

In any standard conductor, the power loss due to resistance heating is given by the following:

$$P_h = I^2 R \ , \tag{6}$$

where

P_h = heat generated due to resistance heating (W)
I = current in conductor (A)
R = resistance of conductor (W, Ω).

A given conductor has a resistance given by the following:

$$R = \frac{\rho L}{A} \ , \tag{7}$$

where

R = resistance of conductor (W, Ω)
ρ = resistivity of conductor (W·m, Ω·m)
L = length of conductor (m)
A = cross-sectional area of conductor (m^2).

This yields the following:

$$P_h = \frac{I^2 \rho L}{A} \ . \tag{8}$$

To reduce the net power lost to conductor heating, which ultimately represents reduced overall part heating efficiency, conductors should be as short as possible and have as great a cross-sectional area as possible. Given that RF coils need to be compact to couple most efficiently with the sample being heated and must also have a fairly complex shape, there is a tradeoff between conductor cross-sectional area and coil geometry.

In addition, RF power is produced via alternating current, which drives the majority of the current in the relatively thin outer surface of the conductor due to the 'skin effect,' which can be expressed as follows:

$$S = \frac{R_{\mathrm{AC}}}{R_{\mathrm{DC}}} \ , \tag{9}$$

where

S = skin-effect ratio, the ratio of the AC current resistance versus DC current resistance
R_{AC} = resistance of conductor when carrying AC current
R_{DC} = resistance of conductor when carrying DC current.

This effectively reduces the conductor cross-sectional area, thus increasing the power lost to conductor heating.

Skin effect in tubular copper conductors is a function of the thickness of the wall of the tube and the ratio of that thickness to the tube diameter. For a given cross-sectional area it can be reduced by increasing the tube diameter and reducing the wall thickness, as shown in figure 17, where f is the frequency of alternating current (Hz) and $R_{0_{1,000\,m}}$ is the resistance of 1,000 m of conductor (Ω).[6]

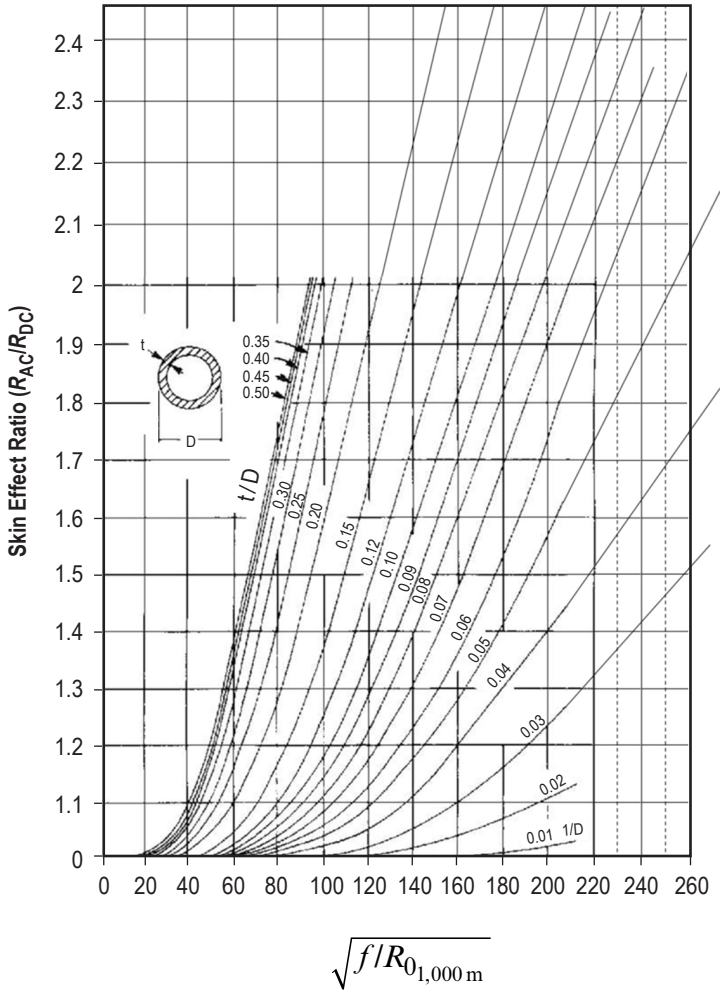

Figure 17. Skin effect for rods and tubes.

A spreadsheet model was set up using these governing equations to produce a summary of expected heat loss due to high-frequency current flow in copper tubing conductors. The model was originally produced to adequately size the recirculating water chiller intended to maintain safe operating temperatures. Given that the maximum possible current flow available from the power supply is 2,400 A, the smallest reasonable coil tubing size and typical operating frequency was selected, yielding 11,215 W of waste heat generated. Table 4 summarizes the various models analyzed, showing clear gains when tube size was increased.

Table 4. Summary of waste resistance heating in conductors.

Geometric Property	Baseline 3/8-in Tubing	Worst-Case Maximum Current	Reduce Frequency	1/2-in Tubing	5/8-in Tubing	3/4-in Tubing
D, copper tube diameter (in)	0.375	0.375	0.375	0.5	0.625	0.75
t, copper tube wall thickness (in)	0.032	0.032	0.032	0.032	0.035	0.035
t/D	0.85	0.85	0.85	0.064	0.056	0.047
I, current in conductor (A)	1,700	2,400	1,700	1,700	1,700	1,700
R_0, DC resistance per unit length (W/mm)	7.55×10^{-7}	7.55×10^{-7}	7.55×10^{-7}	5.53×10^{-7}	4.01×10^{-7}	3.31×10^{-7}
f, frequency of RF (kHz)	24.3	24.3	20	20	20	20
$\sqrt{f/R_{0_{1,000\,m}}}$	179.4	179.4	162.7	190.1	223.2	245.7
S_r, skin effect ratio	1.88	1.88	1.69	1.72	1.88	1.85
AC resistance versus baseline (%)	100	100	91	88	79	78
Heat generated (W)	5,628	1,116	5,059	3,773	2,626	2,429
Waste heat versus baseline (%)	100	199	90	67	47	43

4.4.3 Radio Frequency Heating Coil Field Modeling

Quickfield™ finite element analysis modeling software was used to simulate RF field shape and relative strength for the purposes of optimizing part heating while minimizing stray heating of surrounding hardware. The goal of this modeling was specifically to identify coil and power feed geometric configurations that concentrated heating most effectively within the limitations of fabrication using soft-temper copper tubing (shown in fig. 18).

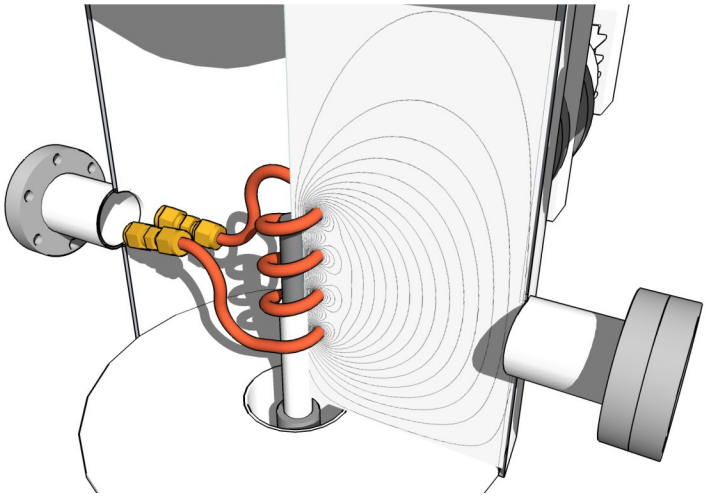

Figure 18. Radio frequency field model for a 1 1/4-in-diameter by 4-in-long heating coil fabricated out of 1/4-in-diameter copper tubing.

Radio frequency field modeling was used primarily to gauge relative improvements based on initial, well-known hardware geometry; i.e., hardware was built and tested, and then an analytical model produced that closely matched that hardware configuration (shown in fig. 19).

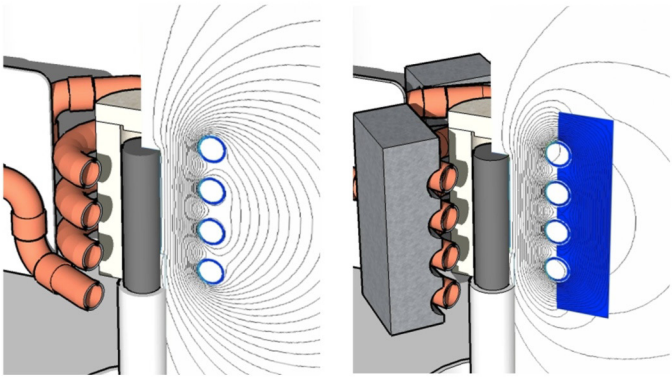

Figure 19. Radio frequency field models showing (a) baseline configuration and (b) baseline with flux concentrators.

Changes made to the geometry of the model were then rapidly evaluated using analysis to obtain new expected performance predictions. In this fashion, the best overall contributions to hardware performance were evaluated and implemented with high confidence, as summarized in table 5.

Table 5. Performance improvement summary from RF modeling.

Comparison	Baseline (W)	With Change (W)	Predicted Improvement (%)
Round tube to rectangular tube	268	266	–1
Reduction of coil diameter	268	397	48
Reduction of coil pitch	268	405	51
Reduction in number of coil turns	268	230	–14
Reduction of coil diameter and pitch	268	814	204
Reduction of coil diameter, pitch, and number of coil turns	268	500	87
Increase in output frequency	268	322	20
Addition of Fluxtrol magnetic field concentrator	268	312	16
Addition of Fluxtrol reduction of coil pitch	268	674	151

4.4.4 Experimental Hardware

4.4.4.1 Test Chamber. The chamber was originally built for doing high-temperature materials compatibility verification testing for the Jupiter Icy Moons Orbiter program.[7] The idea was to perform accelerated life testing (e.g., higher than normal temperatures, higher concentration of impurities, possibly thermal cycling) on different materials and material bonds in helium and xenon gas.

The chamber was assembled from 304 stainless steel tube and standard vacuum Conflat half-nipples and oriented vertically. A single 10-in-diameter Conflat flange at the top of the chamber provided physical access to the RF heating coil for adjustments and replacement. Two 6-in-diameter Conflat flanges were positioned across from each other near the bottom of the chamber. A single 4-in-diameter Conflat flange at the bottom of the chamber provided access to the fuel element sample with minimal chamber disassembly. Several 2.75-in-diameter Conflat flanges were available for roughing pump connection, vacuum measurement, and optical flanges for pyrometer use.

4.4.4.2 Radio Frequency Power Supply. The RF power supply was a 15-kW Flexitune™ model 2-255750-001 solid state converter, shown in figure 20.

It operated at an output frequency of 20–60 kHz at 150 V/2,400 A. The power supply output power was user adjustable down to a minimum of 10% of maximum power or 1,500 W. For power levels below 1,500 W, a custom circuit was designed to provide on/off cycling of power at user-selectable intervals, simulating a variety of duty cycles.

Figure 20. Flexitune +15, 15 kW, 20–60 kHz RF power supply.

4.4.4.3 Water-to-Water Heat Exchanger. The water-to-water heat exchanger was a custom PolyScience recirculator model LL70, shown in figure 21. It incorporated a water pump that cycled conductivity-controlled water through the RF power supply and back to a heat exchanger, where heat was extracted to the laboratory facility water. This process is shown schematically in figure 22.

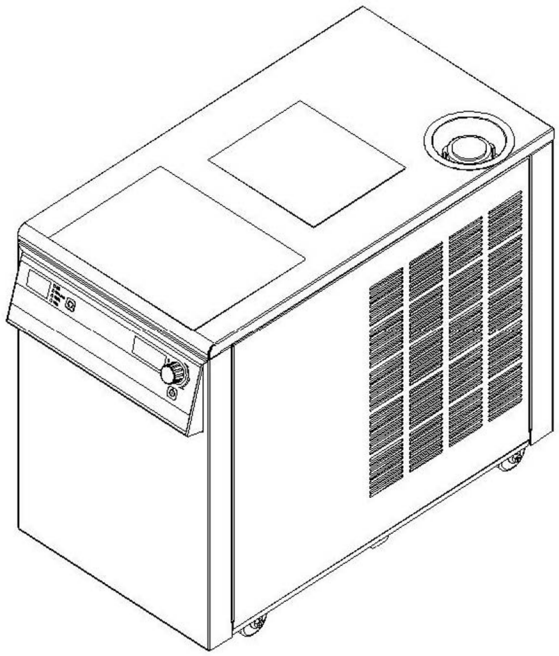

Figure 21. Polyscience recirculating water-to-water heat exchanger.

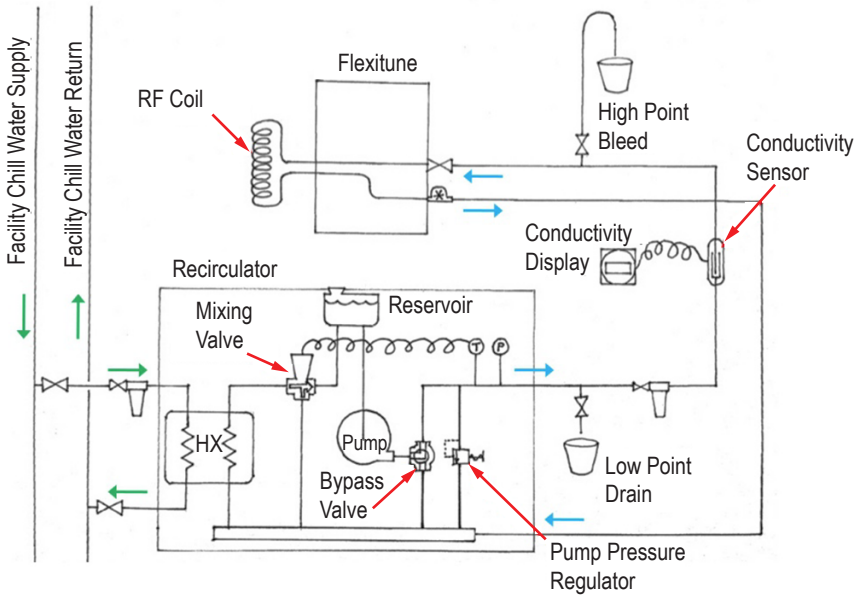

Figure 22. Cooling water flow schematic.

4.4.4.4 Radio Frequency Coil. The RF coils, shown in figure 23, were hand turned from bendable copper refrigeration tubing to appropriate dimensions for testing. Dimensions were typically a tradeoff between RF operating frequency and enclosed fuel element dimensions.

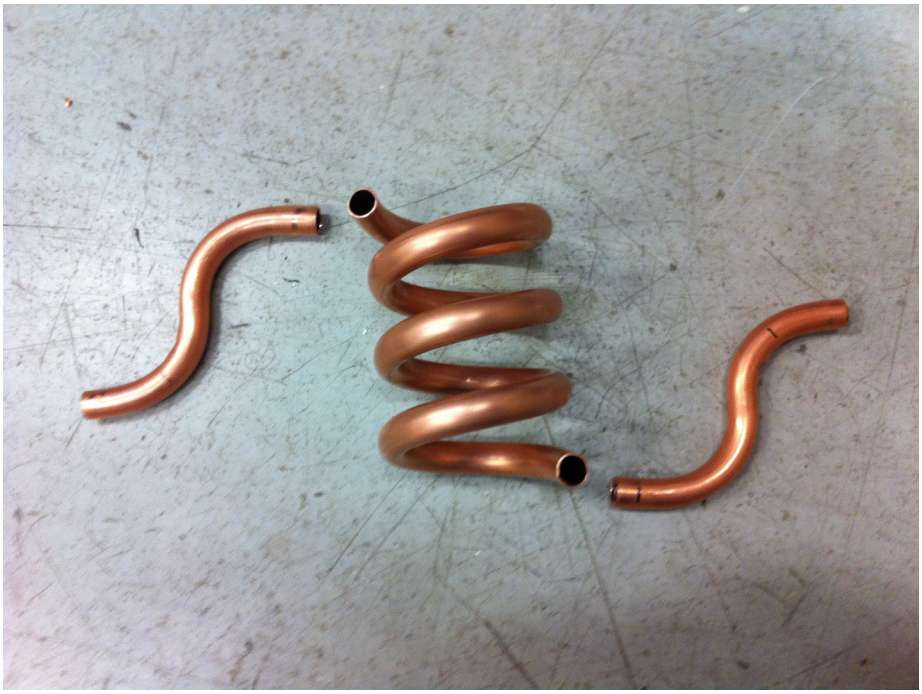

Figure 23. Hand-turned RF heating coil, 3/8-in-diameter tubing.

In general, induction coils were fabricated and installed for testing. If an RF coil combined with the power supply at a resonant frequency outside of the operating range of the power supply, tuning capacitors were available for minor adjustments. If adjustments to the tuning capacitance failed to bring the resonant frequency within the operating range of the power supply, the heating coil properties were required to change. Typically, this amounted to adjusting the number of turns, the turn spacing, and the diameter of the turns, using the following equation:

$$L = \frac{\mu_0 \mu_r N^2 A}{l} \ , \tag{10}$$

where

L = inductance (H)
μ_0 = permeability of free space, $4 \cdot \pi \times 10^{-7}$ H m^{-1}
μ_r = relative permeability of core material
N = number of turns
A = area of cross section of the coil (m^2)
l = length of coil (m).

In general, greater fuel element heating depth is obtained with lower frequencies. Therefore, to achieve volumetric heating more typical of a nuclear fuel element, lower frequencies were desired. At extreme limits of the power supply frequency range, however, power limiting could occur. Thus, the best-case scenario for maximum available heating power was to operate at the middle of the power supply's frequency range. Radio frequency coils were therefore fabricated so that a resulting operating frequency between 20 and 40 kHz was obtained.

Radio frequency coils were fabricated from relatively thin-walled copper tubing. Alternating current flowed through the outermost layer of the tube due to skin effect. The effective resistance was very high and produced high-resistance heating rates that must be absorbed by water flowing through the tubing. The waste heat can be reduced by moving to larger diameter tubing. The tradeoff laid between ease of compact coil fabrication (smaller diameter tubing) and reduction of ohmic heating (larger diameter tubing). Additionally, greater cooling water flow capacity was available with larger diameter tubing. The different coils used are shown in figure 24, while their dimensions and operating frequencies are shown in table 6.

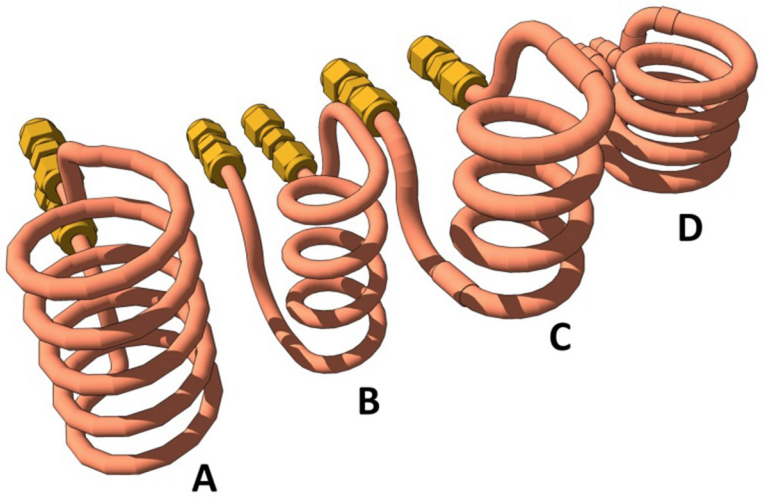

Figure 24. Different coils installed for testing.

Table 6. Radio frequency heating coil dimensions, operating frequencies, predicted and observed.

Coil	Tube Size (in)	Coil Diameter (in)	No. of Turns	Length of Coil (in)	Calculated Inductance (μH)	Turning Capacitance (μF)	Estiated Resonant Frequency (kHz)	Operating Frequency As Tested (kHz)
A	0.25	2	5	4	0.51	3.3	22.7	21.2
B	0.25	1.25	4	2.8	0.14	3.3	28.1	25
C	0.375	1.875	4	3	0.37	3.3	25.7	27.3
C	0.375	1.875	4	3	0.37	5.3	20.3	21.7
C	0.375	1.875	4	3	0.37	5.9	19.2	20.3
D	0.375	1.875	4	1.75	0.54	5.3	23.3	22.9
D	0.375	1.875	4	1.75	0.54	5.9	22	21.5
E	0.5	2	4	1.97	0.56	6.6	20.6	*

*This coil not yet tested but planned for future testing.

5. TEST RESULTS

5.1 Melting Test

After preliminary checkout testing, which confirmed operation of the RF power supply and basic functionality of the optical pyrometers, a melting test using a 308 stainless steel dummy sample was performed. (The sample is shown before and after melting in fig. 25.) The melting point of the stainless steel was ≈1,500 °C, which provided a general calibration confirmation for the pyrometers. Pyrometer temperature measurements were observed in parallel with visual observation of the dummy sample. With melting observed by sight, RF power was discontinued and pyrometer output temperature recorded. Testing was conducted safely after clearly investigating and documenting hazards via job hazard analysis (JHA). The detailed JHA can be found in appendix F. All gas handling hardware was specified to ensure safe operations.

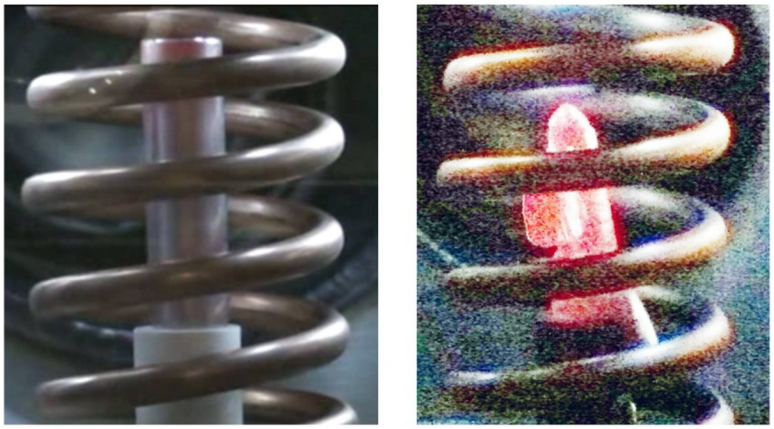

Figure 25. Sample of 308 stainless steel before and after melting at 1,450 °C.

A rough estimation of overall RF heating efficiency was made based on raising the sample temperature from 25 °C (room temperature) to 1,500 °C (sample melting point) as summarized in table 7.

Table 7. Radio frequency coupling efficiency estimation during stainless steel melt test.

50	Duration of applied RF (s)
9.3	Power output level indicated on Flexitune (kW)
465	Total energy input (kJ)
25	Fuel element start temperature (°C)
1,500	Fuel element end temperature (°C)
0.5	Specific heat of fuel element, *Cp* (kJ/kg·K)
8.03	Fuel element density, ρ (cm^3)
6.43518	Fuel element volume, *V* (cm^3)
51.6745	Mass of fuel element, *m* (g)
38.11	Total energy added to fuel element (kJ)
8.2	Overall efficiency of RF heating (%)

5.2 Low-Power Heating Tests

To achieve maximum possible fuel element temperatures, an effort was made to reduce radiation heat transfer from the fuel element to the vacuum chamber wall. That loss mechanism was the primary heat loss path. The use of a high-temperature ceramic insulator located between the RF coil and the fuel sample was evaluated by test.

A baseline heating test was devised for use in comparing the effectiveness of different element insulation schemes. The RF power supply supplied 1.5 kW for each test, heating a 308 stainless steel sample to 1,200 °C or a steady state temperature, whichever was lowest. This resulted in a recorded heating profile and subsequent cooling profile that was visually compared, test to test, to provide qualitative results.

Data were recorded for four separate tests: (1) Heating sample at 1.5 kW without insulation, vacuum pumps isolated, (2) heating sample at 1.5 kW with insulation, vacuum pumps isolated, (3) heating sample at 1.5 kW with insulation, vacuum pumps operating, and (4) heating sample at 1.5 kW without insulation, vacuum pumps operating.

The heating profiles shown in figure 26 clearly indicate that, for the temperature regime of 600 to 1,000 °C, no appreciable gain in heating efficiency was obtained by the inclusion of a ceramic insulator between the RF coil and the fuel element. In addition, these profiles underscore the importance of fully baking out ceramics prior to use—the release of volatiles upon heating is shown by the dotted line, which varies considerably during heating when compared to the other three tests.

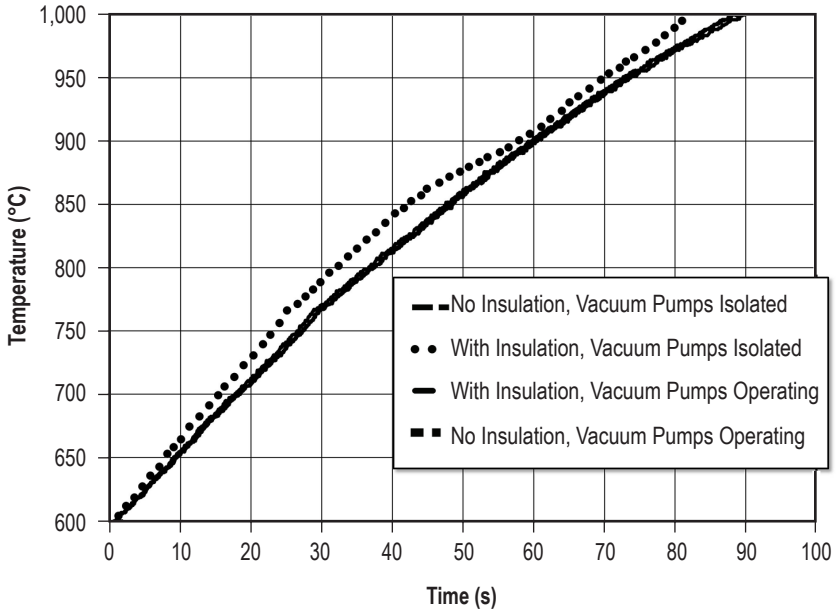

Figure 26. Low-power heating tests fuel element temperature profile during heating, 600 to 1,000 °C.

In the heat loss temperature profile in figure 27, the effectiveness of the insulator can be seen. In both cases in which an insulator was used, the rate of heat loss was noticeably reduced. It should also be noted that, as the quality of vacuum dropped (as is the case when vacuum pumps are isolated), a greater heat loss rate resulted.

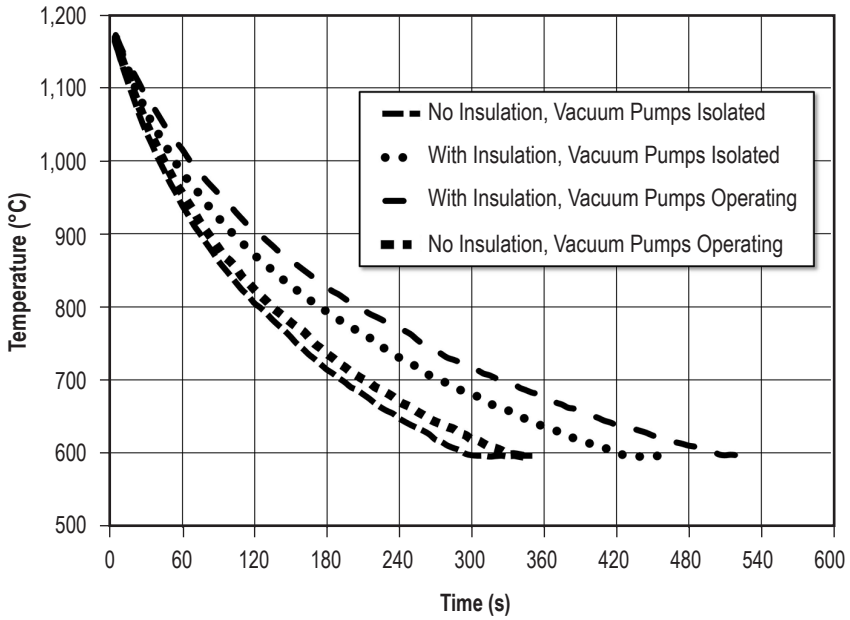

Figure 27. Low-power tests fuel element temperature profile during cooling, approximately 1,200 to 600 °C.

The best results for maximum element temperature were expected when maintaining the deepest possible vacuum combined with the use of an insulator between the RF coil and the fuel sample.

5.3 In-Coil Insulator Evaluation

Analytical modeling and operational testing indicated that the primary heat loss mechanism from the heated sample was thermal radiation. High-temperature insulation materials were employed to fabricate insulators to fit over the samples but still fit inside the RF heating coil, as shown in figure 28.

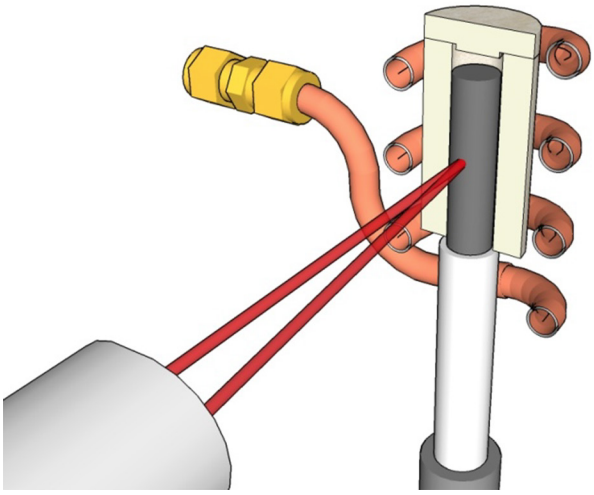

Figure 28. In-coil insulator arrangement.

The insulator material property requirements were as follows: high-temperature resistance, electrical resistance, and little-to-no magnetic susceptibility. In general, these parameters led to materials that were transparent to RF radiation, allowing the samples to be heated through the insulation. Additionally, there were four different materials tested for use as in-coil insulators, as shown in figure 29: alumina, zirconia, graphite foam, and BN.

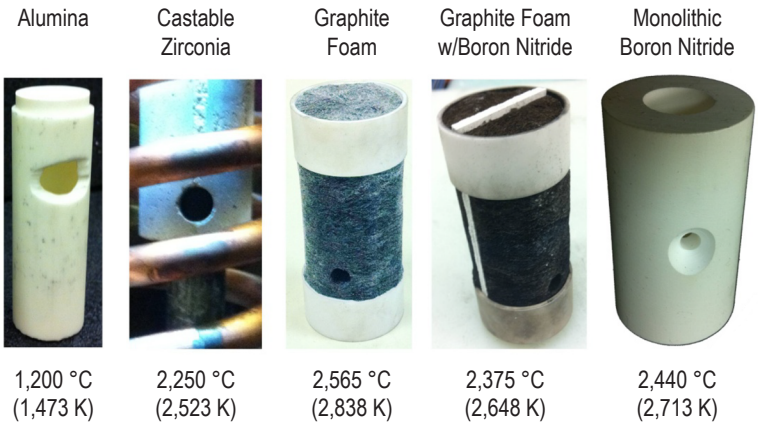

Figure 29. In-coil insulator performance summary.

A small, thin-walled tube of alumina was available and modified to provide a viewing port for the pyrometer. Testing of the alumina insulator, as shown in figure 30, demonstrated that losses from the heated element were reduced when using an insulator. However, the very thin wall of the alumina insulator limited its effectiveness. As a result, zirconia ceramic was used for follow-on tests.

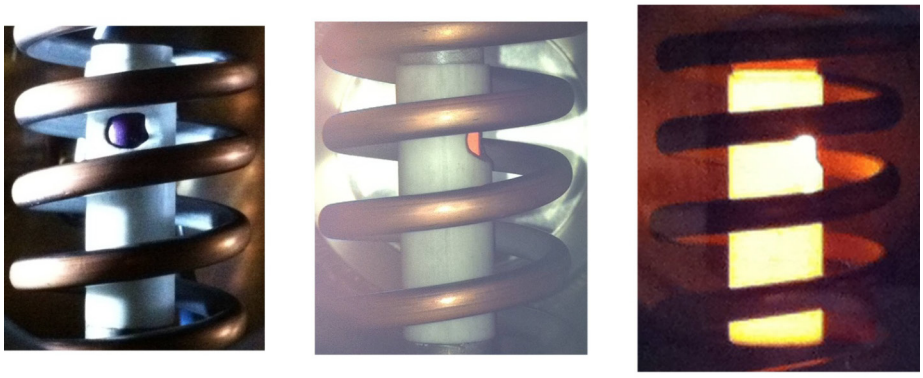

Figure 30. Alumina insulator radiating heat from enclosed sample during test.

To maximize available insulation for a given coil/sample element geometry, parts were cast using custom-made molds. Failure of the zirconia insulators at sample element temperatures of 2,250 °C regardless of fabrication technique led to abandonment of their use. A small sample of graphite foam was installed as an insulator, and dramatic thermal performance improvements were recorded (sample temperature up to 2,565 °C (2,838 K)). The inherent electrical conductivity of the graphite foam was of concern, and testing using BN slivers to break up graphite foam halves was performed, resulting in negative performance improvement. The potential reactivity of the graphite foam in an eventual flowing hydrogen environment led to abandonment of its use. Ultimately, solid h-BN was selected as an optimal insulator material. At this writing, the best performance using BN has been an element temperature of 2,440 °C (2,713 K).

5.4 High-Temperature Hydrogen Flow Testing

During high-temperature hydrogen flow testing, 308 stainless steel samples were installed in the chamber, heated, and exposed to hydrogen gas (fig. 31). These samples were employed primarily to conduct checkout testing of the gas flow system and to step through system operation procedures.

Figure 31. Stainless steel samples after hydrogen tests.

One interesting observation in these stainless steel samples was the apparent melting location at approximately the same elevation as the pyrometer view hole in the h-BN insulator. The tungsten sample was tested per procedures described in appendix G.

After checkout testing was complete a pure tungsten rod sample was installed to conduct maximum power testing with less concern for melting. The tungsten sample was heated to steady state at various RF power levels while flowing 16.5 SLPM of hydrogen gas. The total test duration was ≈55 min during which time the maximum tungsten element temperature was 2,250 °C (2,523 K), as shown in figure 32. The test was terminated with the failure of power fuses in the RF power supply. All other systems checked out and performed as expected.

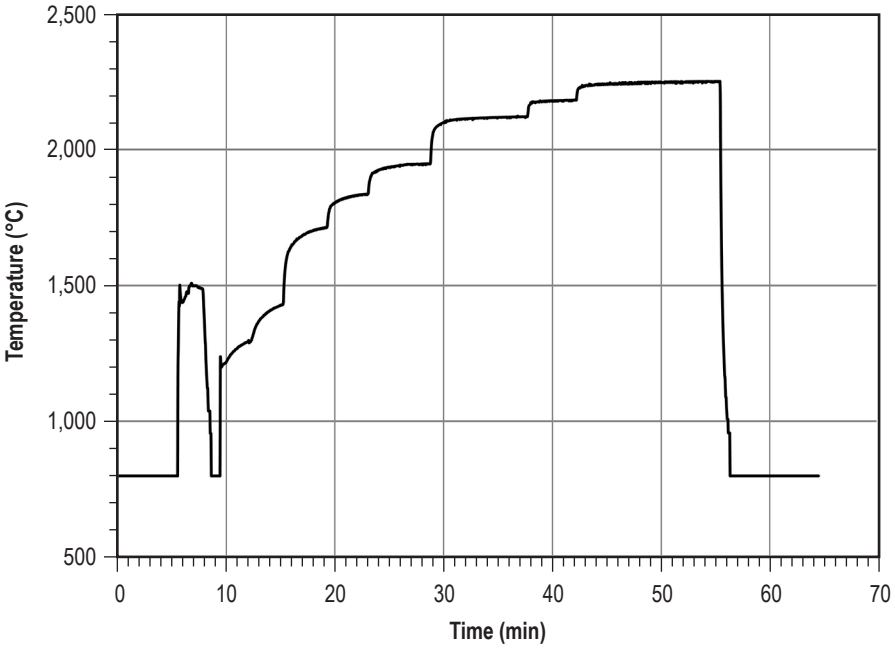

Figure 32. Tungsten temperature versus time during flowing hydrogen test.

6. CONCLUSIONS

CFEET was able to successfully achieve a maximum sample element temperature of 2,250 °C (2,523 K) while flowing hydrogen gas through the sample.

Although the final test was limited in duration, it is expected that tuning of the power supply in conjunction with an upgraded RF coil will allow the power supply to stay well within its operating limits for the testing durations required for adequate sample testing. These testing durations are expected to be as long as 3 hr of continuous operation at high temperature.

The test hardware operates safely and provides a low-cost screening tool for NTR fuel materials and fabrication processes.

Future work includes the buildup of a more efficient heating coil and additional insulation around the sample. Moreover, further testing may employ a molybdenum heat shield located outside of the RF coil but within the chamber.

APPENDIX A—INSTRUMENTATION SCHEMATIC

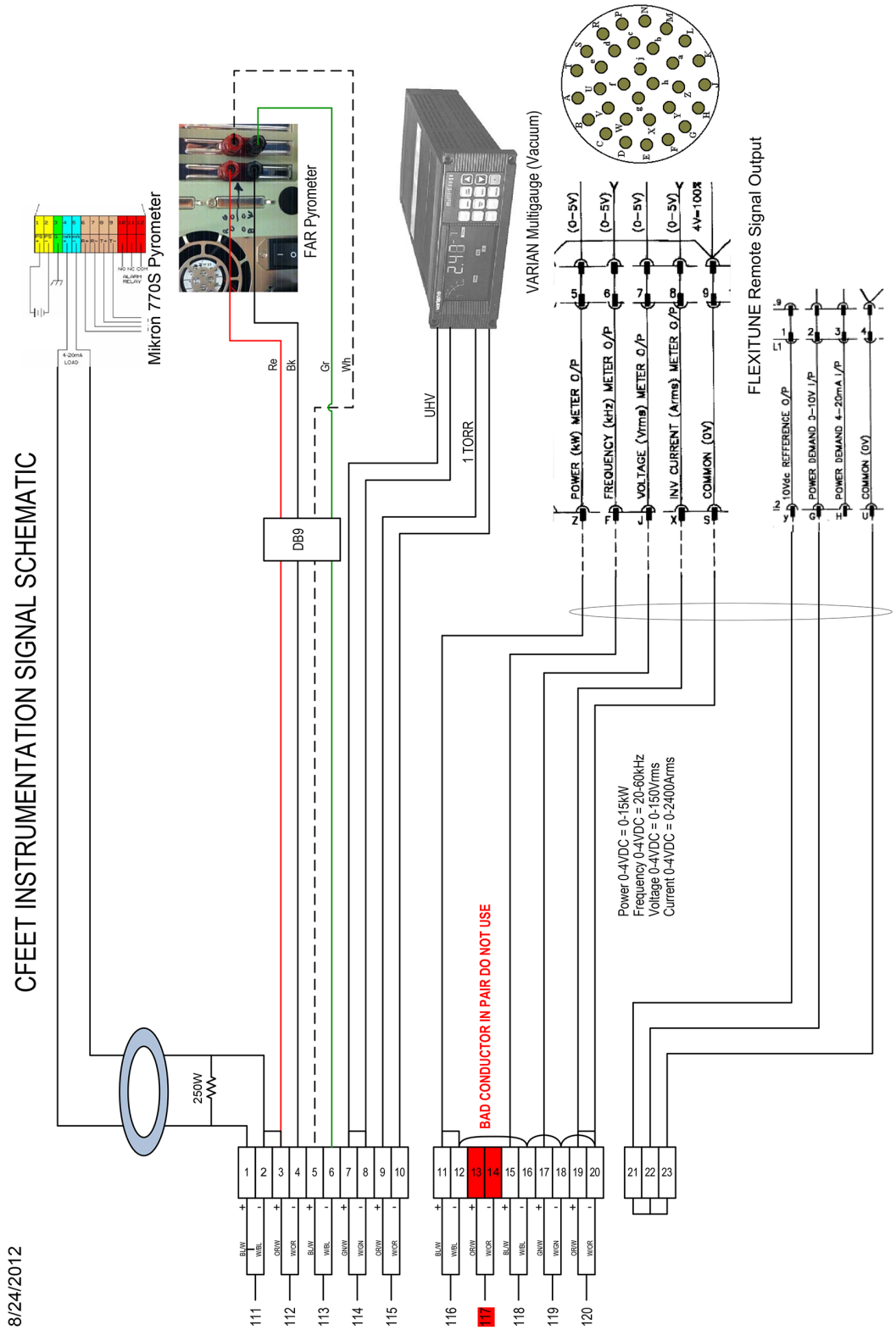

APPENDIX B—WATER SCHEMATIC

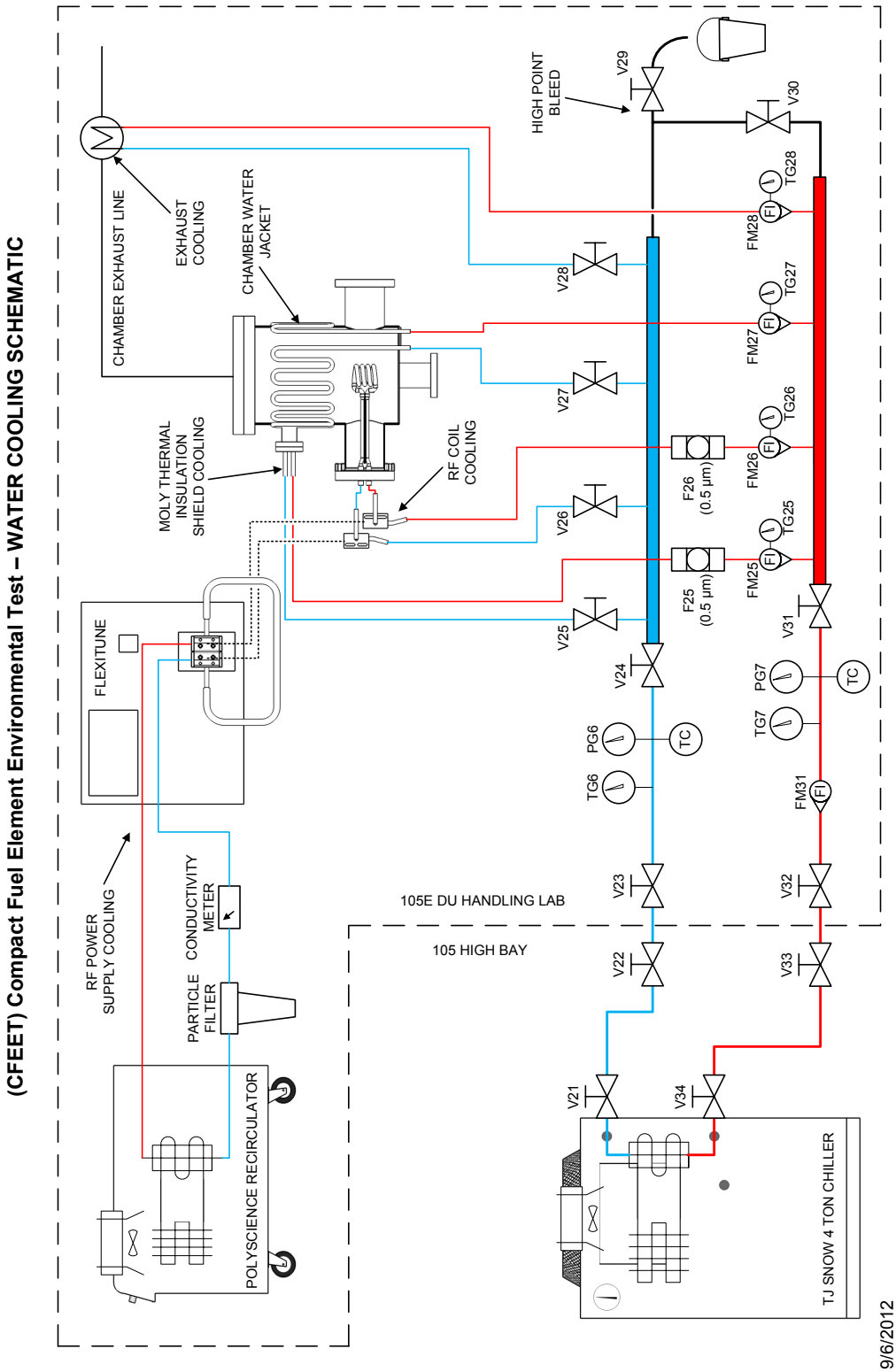

APPENDIX C—GAS SCHEMATIC

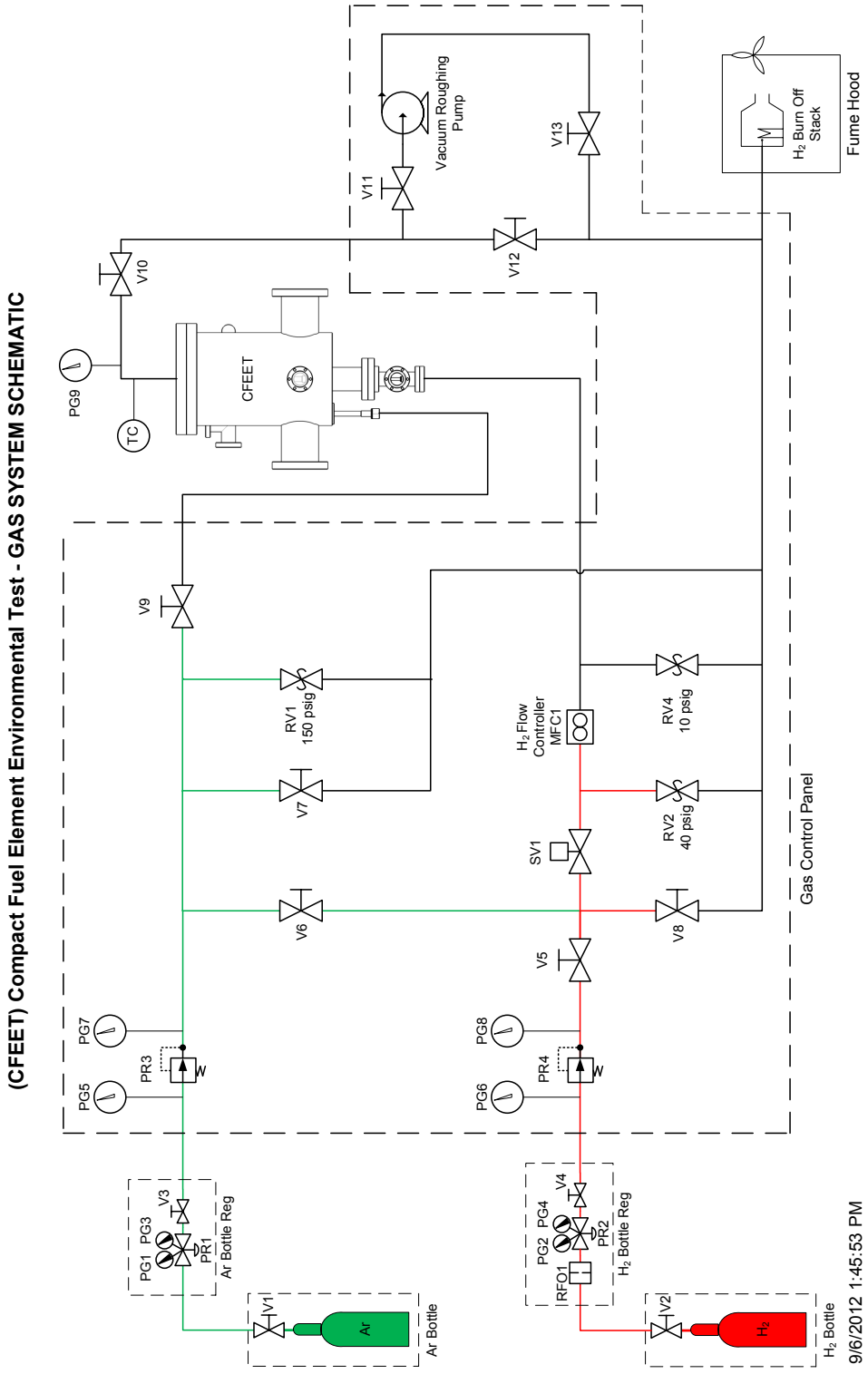

APPENDIX D—COMPONENT DESCRIPTOR LIST FOR GAS SYSTEM SCHEMATIC

Gas System Component List

Comp ID	Size	Component Description	Other info / Description
V1	50L	k-bottle multi-turn isolation valve	k-bottle multi-turn isolation valve, included with rented bottle
V2	50L	k-bottle multi-turn isolation valve	k-bottle multi-turn isolation valve, included with rented bottle
V3	1/4"	Bottle regulator iso valve	Multi-turn Swagelok isolation valve
V4	1/4"	Bottle regulator iso valve	Multi-turn isolation valve
V5	1/4"	Hand valve	Panel-mounted, multi-turn valve
V6	1/4"	Hand valve	Panel-mounted ball-valve, 90° actuation
V7	1/4"	Hand valve	Panel-mounted, multi-turn valve
V8	1/4"	Hand valve	Panel-mounted, multi-turn valve
V9	1/4"	Hand valve	Panel-mounted, multi-turn valve
V10	1"	Hand ball valve	1" ball valve with Swagelok tube fittings, tube mounted
V11	1"	Hand ball valve	1" ball valve with Swagelok tube fittings, panel mounted
V12	1"	Hand ball valve	1" ball valve with Swagelok tube fittings, panel mounted
V13	1"	Hand ball valve	1" ball valve with Swagelok tube fittings, panel mounted
MFC1	1/4"	Mass flow controller	Mass flow controller for H_2
RFO1	1/4"	H_2 flow reducing orifice	H_2 bottle regulator stuck open relief valve
RV1	1/2"	Relief valve	Regulator fails open relief valve Ar
RV2	1/2"	Relief valve	Regulator fails open relief valve H_2
RV4	1/2"	Relief valve	Chamber relief valve H_2 / Ar
SV1	1/4"	H_2 solenoid shut-off valve	H_2 shut-off solenoid valve, controlled by TC at exhaust stack
PR1	CGA 580	Ar bottle regulator	Ar bottle-mounted regulator
PR2	CGA 350	H_2 bottle regulator	H_2 bottle-mounted regulator
PR3	1/4"	Ar panel regulator	Panel-mounted regulator
PR4	1/4"	H_2 panel regulator	Panel-mounted regulator
PG1	1/4"	Ar k-bottle regulator supply pressure gauge	Ar regulator mounted supply gauge
PG2	1/4"	H_2 k-bottle regulator supply pressure gauge	H_2 regulator-mounted supply gauge
PG3	1/4"	Ar k-bottle regulated pressure gauge	Ar bottle regulated output gauge
PG4	1/4"	H_2 k-bottle regulated pressure gauge	H_2 bottle regulated output gauge
PG5	1/2"	Ar panel supply pressure gauge	Panel-mounted 4" gauge
PG6	1/2"	H_2 panel supply pressure gauge	Panel-mounted 4" gauge
PG7	1/2"	Ar panel regulated pressure gauge	Panel-mounted 4" gauge
PG8	1/2"	H_2 panel regulated pressure gauge	Panel-mounted 4" gauge
PG9	1/4"	Chamber vac/pressure gauge	Chamber exhaust mounted on boss, McMaster Carr

APPENDIX E—RADIO FREQUENCY POWER SCHEMATIC

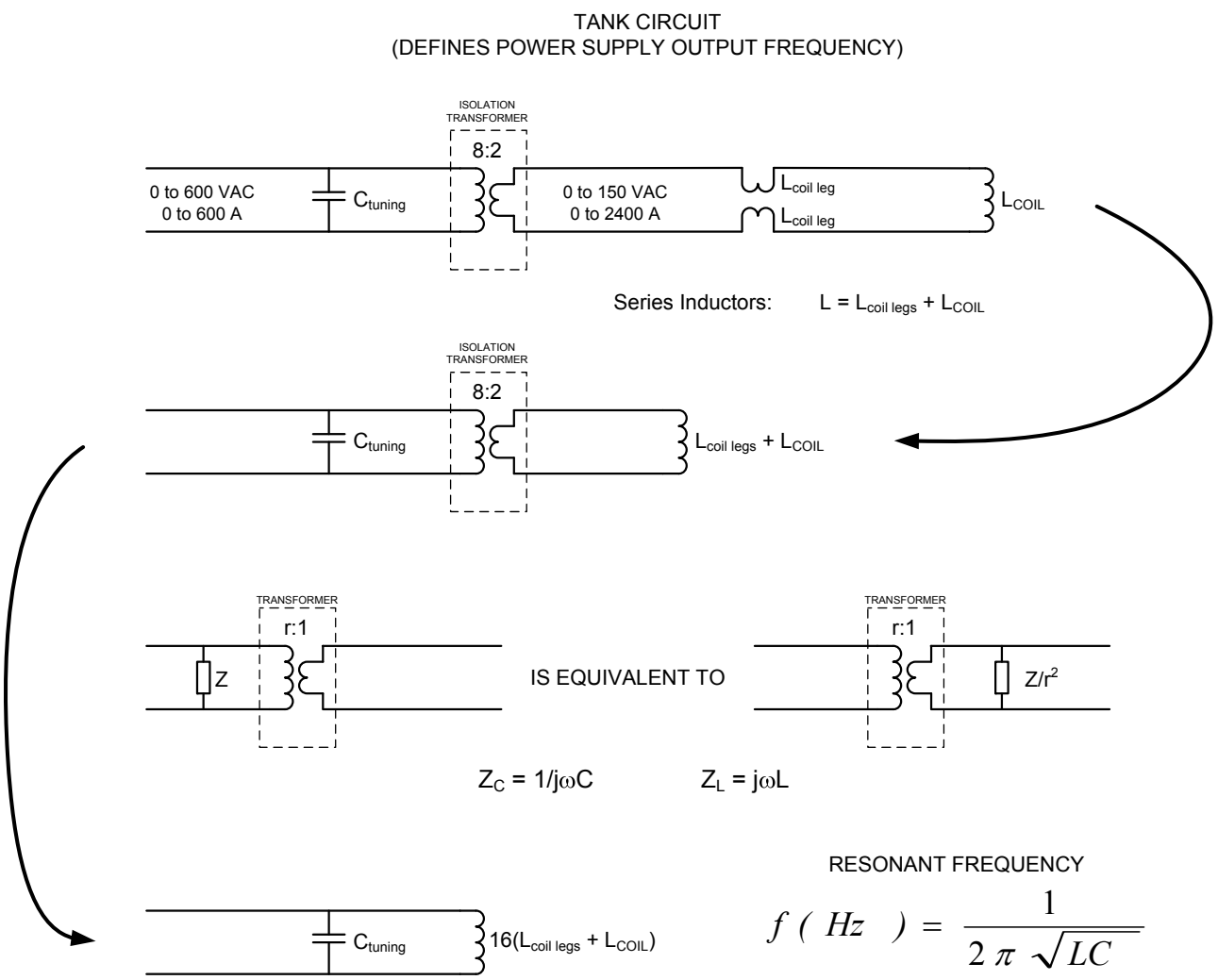

APPENDIX F—JOB HAZARD ANALYSIS

JHA Number (optional): _____

JOB HAZARD ANALYSIS

Workplace/Activity/Job/Operation:			Date:
Operation - Hot Hydrogen Testing of Nuclear Thermal Propulsion Fuel Element Samples			08/20/2012
JHA Performed By:	**Supervisor:**	**Org. Code:**	**Location (Building/Room/Area):**
David Bradley	Jim Martin	ER24	4205/105E

Supervisors ensure the following:

- **Employees review the JHA prior to performing the activity/job/operation for the first time, or when changes are made to the activity/job/operation that affect existing controls, or when they have not performed the activity/job/operation regularly for an extended period of time (approx. 6 months).**
- **Employees sign the signature sheet or other method identified by the supervisor to indicate they understand the hazards/concerns and the actions taken to eliminate/control them.**
- **The JHA is easily accessible to employees. Posting adjacent to the activity/job/operation is one method.**
- **There is a one-to-one relationship between an identified concern/hazard and the actions necessary to control it**

Rationale why this job/task is considered as "low or minimal risk" and not "high or moderate risk" where a more indepth hazard analysis is required. Refer to MWI 8715.15, "Ground Operations Safety Assessment Program" for more information.	List specific Personal Protective Equipment (PPE) and/or training required for this job/task.
During normal operations the operator should not be exposed to purge gas (Argon), reaction gas (H2), high temperature surfaces or harmful levels of non-ionizing radiation. The listed PPE reduces the possibly of injury in the event of off-nominal operations. Engineering Controls include automatic cooling water high temperature shutdown of RF power supply, rated pressure systems, relief valves for protection from pressure and flow, a vent hood is utilized to vent H2 & Ar to the outside, and a H2 burn off stack is utilized to burn vented excess H2. A procedure is also utilized to limit hazards and misuse of equipment.	1. Safety glasses 2. Leather gloves 3. Lab coats or equivalent 4. Dust mask 5. Oxygen detector

Does this JHA serve as the workplace hazard assessment for this activity/job/operation? Yes ☒ No ☐

If this JHA does not serve as the workplace hazard assessment for this activity/job/operation an additional workplace hazard assessment is required. See MWI 8715.4, "Personal Protective Equipment (PPE) and Systems" and 29 CFR Part 1910.132(d).

No.	Steps containing the potential to create a hazard	Description of the hazard (Be specific)	Action to eliminate/control the hazard (Be specific)
1	Gas flow operation.	H2 Mass flow controller failure in the stuck open position.	Disrupt power to the controller by pressing the switch on the power strip and close the gas bottle supply valves. If pressure exceeds 10 psig pressure relief valves open and vent to the burn stack in the fume hood.
2	Gas flow operation.	Failure of a seal during operation creating a potential asphyxiation hazard from accidental gas release.	Close H2 bottle valve and flow Ar util burn-stack flame extinguishes. Distrubt power to RF power supply. Allow cool to room temperature and evacuate the lab to promote ventilation through the fume hoods before initiating repair. Wear PPE 5.
3	Gas flow operation.	Chamber over-temperature as determined by the data acquisition system or non-contact IR temperature probe. Desired operating temp of sample is 3000 K, max chamber temp is 150 C.	Chamber over-temp not a major concern since the vessel is water jacketed and the heated sample is highly insulated If chamber temp = max temp decrease power supply setting. If ineffective, deactivate the RF power supply. Allow chamber to cool to room temp. Wear PPE 1-3.
4	Flowing H2 through the chamber.	H2 leak of sufficient quantity that leads to a potential ignition situation	Evacuate system to remove contaminants and to perform a leak check using a helium leak detector before initiating operations per "Evacuation and Leak Detection" procedures. Ensure possible ignition sources are not near H2 flow lines. H2 monitors are placed adjacent to H2 lines.

JHA Number (optional): _____

JOB HAZARD ANALYSIS
(Continuation Sheet)

No.	Steps containing the potential to create a hazard	Description of the hazard (Be specific)	Action to eliminate/control the hazard (Be specific)
5	Removing tested samples	Contacting hot surfaces	Allow chamber to cool to room temperature as verified by the DAQ display and/or hand-held IR temperature probe initiating sample retrieval operations as desribed in "Shut-down proceedures". The chamber is water jacketed and acts as a protective barrier to prevent burns by direct contact with the chamber inner wall. Wear PPE 1-3.
6	Removing tested samples	Fracture of insulation tube creating a cutting hazard and a potential powder inhalation hazard.	Wear PPE 1-4.
7	Gas flow operation	Pressure relief valve activation	The Low Pressure Relief valve (RV) is down-stream of the H2 mass flow controller. This RV activates at 10 psig and has a max flow rate of 51 SLPM. The RV up-stream of the H2 mass flow controller activates at 40 psig. The RV up-stream of the Ar control valve activates at 150 psig. These up-stream RVs have a max flow rate of 51 SLPM, to protect against supply regulators stuck open flow of approximately 40 SLPM. All RVs exhaust to the H2 burner in the fume hood. Typical filament flame size is 6-10 inches. The fume hood interior is stainless steel and capable of withstanding burn-off flames. If down-stream RVs activate the operator will decrease the H2 mass flow controller settings or throttle the Ar purge valve to decrease pressure. If up-stream RVs activate the operator will decrease H2 and N2 regulator valves to decrease pressure. If ineffective, the operator will close H2 and Ar supply valves. If ineffective, operators will evacuate the room. At no time is the experiment left unattended during operation.
8	Gas flow operation	H2 burn-off filament "flame out"	At maximum H2 flow rates conventional flame systems can flame out. However, using a resistive heating filament allows for H2 to combust once in the vicinity of the heated filament. A thermocouple detects flame at the exhaust and a controller automatically shuts off hydrogen flow via SV1 in the event of "flame out."
9	Gas flow operation	Pressure system rupture	The maximum pressure in the system consists of the 3000 psig Argon bottle and 2200 psig H2 gas bottle; however, the system is operated at much lower pressures. The first and second stage regulators drop the pressure down to < 10 psig. A components list with associated pressure ratings is provided in the procedural document. All gas components meet operating requirements of 10 psig. Exceeding 10 psig will activate the RV down-stream of the mass flow controllers. Exceeding 40 and 150 psig will activate the H2 and Ar RVs up stream of the mass flow contoller/control valve, respectively.

JHA Number (optional): _____

JOB HAZARD ANALYSIS
(Continuation Sheet)

No.	Steps containing the potential to create a hazard	Description of the hazard (Be specific)	Action to eliminate/control the hazard (Be specific)
10	Gas flow operation	Flame traveling down the burn-off stack	A flame arrestor (inconel mesh) is place at the outlet of the H2 burn -off stack that prevents migration of the flame from the filament.
11	Flowing H2 through the chamber.	H2 monitor failure during operations	H2 monitors are calibrated at appropriate intervals and batteries have sufficient charge to meet expected duty cycle requirements. Periodically check H2 monitors during operation to verify functionality. H2 monitors are placed near the H2 supply lines for effective functionality as in "Initialization procedure".
12	Gas flow operation	Combustion of H2 in the flow lines	The system is evacuated to 30 mmHg to remove air from the system, then is purged with Argon to displace trace oxygen contaminants. This ensures that any free H2 will only combust when it reaches the H2 burn-off stack filament.
13	Operation of RF heating.	Exposure to non-ionizing radiation.	Persons possessing electronic pace-makers are not allowed in the vicinity of the testing hardware during operation. Warning signs posted prominently at entrance to room.
14	Operation of RF heating.	Exposure to high current electrical terminals.	All electrical terminals will be sufficiently insulated to prevent accidental contact during operation.
15	Operation of RF heating.	Loss of cooling water to power supply.	RF power supply is equipped with both high water temperature and loss of flow automatic shut-offs to deactivate power supply in the event of cooling water loss.
16	Gas flow operation.	Operator asphyxiation due to leak of nitrogen or hydrogen gas.	Operator must wear PPE 5, oxygen detector, while operating CFEET hardware. Room is also equipped with a wall-mounted oxygen sensor.

JHA Number (optional): _____

JOB HAZARD ANALYSIS
(Continuation Sheet)

Page _____ of _____

No.	Steps containing the potential to create a hazard	Description of the hazard (Be specific)	Action to eliminate/control the hazard (Be specific)

JHA Number (optional): _____

EMPLOYEE SIGNATURE PAGE

Job/Task Name or Description:
Operation - Hot Hydrogen Testing of Fuel Element Samples

Location (Building/Room/Area):

No.	Employee Name (print)	Employee Signature	Org Code	Date
1.	Jim Martin		ER24	08/20/2012
2.	David Bradley		ER24	08/20/2012
3.	Omar Mireles		EM32/ER24	08/20/2012
4.				
5.				
6.				
7.				
8.				
9.				
10.				
11.				
12.				
13.				
14.				
15.				
16.				
17.				
18.				
19.				
20.				
21.				
22.				
23.				
24.				

APPENDIX G—TEST PROCEDURES

Compact Fuel Element Environmental Simulator (CFEET) Procedures

Authors:

_____

Omar Mireles
NASA MSFC – Advanced Propulsion Branch

_____

David Bradley
Yetispace Inc. – Advanced Propulsion Branch

Concurrence:

_____

Robert Hickman
NASA MSFC – Materials and Joining Branch

_____

Jim Martin
NASA MSFC – Advanced Propulsion Branch

_____

Alvin Eidson
NASA MSFC – Industrial Safety Engineering Lead

Revision	Description	Date
0	Original issue	02 March 2012
1	Procedural Update	14 March 2012
2	Design Modification Update	11 June 2012
3	Design Modification Update	20 August 2012

SAFETY PRECAUTIONS and WARNING NOTES

Note: Information requiring special emphasis
***Caution*:** An item that if not executed properly can lead to damage of hardware
WARNING: An item that if not executed properly can lead to severe damage of hardware, injury, or loss of life

If actions do not proceed as planned, cease action, and notify: David Bradley at 256.544.4334 or Omar Mireles at 256.544.6327

SUPPLEMENTAL INFORMATION

Photographs, diagrams, schematics, and tables with detailed specifications are located in the appendix and are meant to supplement operational steps.

Access Control

Building 4205/room 105 has key card readers to allow access to authorized personnel only. Room 105E has keys issued to required personnel only. Ensure the doors are closed and locked before conducting operations.

PPE

During CFEET operation, safety glasses, a lab coat or equivalent and leather working gloves should be worn in the event of a cooling system or gas system leak or when handling hot surfaces or sharp items. Oxygen detectors will be used to guard against the asphyxiation hazards of the Argon purge gas system and include a fixed room oxygen monitoring system and a portable oxygen detector clipped to the system operator. Hydrogen detectors will be in place to detect potential hydrogen leakage.

Operation Specifics

This process requires manual operation and is at no time intended to be left unattended. This activity is conducted in the processing lab (4205/105E). NTP candidate fuel samples are inductively heated to between 2700 and 3000 K in a vacuum chamber. Low pressure (<10psig) Hydrogen then flows through the sample in order mimic NTP environmental conditions. Samples undergo environmental exposure for a series of pre-determined durations in order to observe fuel performance and possible decomposition. The heated hydrogen gas is then cooled in an expansion space. The chamber exhaust section ends with a coarse mesh filter where the remaining hydrogen gas is flowed through a SiC igniter into a fume hood.

`

GLOSSARY OF TERMS

°C	Degrees Celsius
Ar	Argon
CCW	Counter Clock Wise
CFEET	Compact Fuel Element Environment Test
CW	Clock Wise
DAQ	Data Acquisition System
F	Filter
FM	Flow Meter
g	Gram
H_2	Hydrogen
inHg	inches of mercury
JHA	Job Hazard Analysis
K	Kelvin
LEL	Lower Explosive Limit
MFC	Mass Flow Controller
mmHg	millimeters of mercury
NTP	Nuclear Thermal Propulsion
PG	Pressure Gauge
PID	Proportional, Integral, Derivative
PPE	Personnel Protective Equipment
PR	Pressure Regulator
psig	Pounds per square inch gauge
RF	Radio Frequency
RFO	Flow Reducing Orifice
RV	Relief Valve
SCCM	Standard Cubic Centimeters Per Minute
SiC	Silicon Carbide
SLPM	Standard Liters Per Minute
SV	Solenoid Valve
TC	Thermocouple
TG	Mechanical Temperature Gauge
V	Valve
VAC	Volts AC

INITIALIZATION

1. Experiment data sheet – Prepare

2. ALL VALVES – CLOSE

3. ALL REGULATORS – FULL CCW

4. Vacuum chamber – Inspect for damage
   Note: If damaged repair then proceed with next step

5. Fuel element sample – Load onto the pedestal

6. BN insulator – Install around the sample

7. Chamber top gasket – Install

8. Chamber top flange – Install

9. 480 VAC power cord for RF power supply – PLUG IN

10. 208 VAC power cord for RF power supply chill water Recirculator – PLUG IN

11. 110 VAC power cords for instrumentation and vacuum pumps – PLUG IN

12. 110 VAC power cords for mass flow controllers and solenoid valve control system – PLUG IN

13. 230 VAC power cord for RF coil and chamber cooling water Recirculator (located in 105 high bay outside of 4205/105E processing lab) – PLUG IN

14. H_2 mass flow controller set point – 0.0 SLPM

15. RF power supply water cooling pump – ON

16. RF coil and chamber cooling water cooling pump – ON

17. DAQ system – ON

18. FAR pyrometer – ON

19. H_2 monitors – ON
    Note: Place monitors adjacent to H_2 lines.
    Note: Monitors should read 0% LEL. If not, calibrate according to the manual.
    Note: Batteries should be charged to meet expected duty cycle
    Note: Periodically check monitors during operation to verify functionality.
    Note: Ensure possible electrical ignition sources are not adjacent to H_2 lines.

20. Portable oxygen monitor – ON
    Note: Clip oxygen monitor to operator lab coat or equivalent.
    Note: Room oxygen monitor is automatic and requires no operator input.

21. Don PPE including lab coat or equivalent, safety glasses, and leather gloves

22. V1 (Argon bottle valve) – OPEN

23. set PR1 (Argon bottle regulator) to 50 psig

24. V3 (Argon bottle regulator iso valve) – OPEN
    Note: Verify pressure at PG5 on front of gas panel.

25. V2 (Hydrogen bottle valve)– OPEN

26. Set PR2 (H_2 bottle regulator) to 50 psig

27. V4 (Hydrogen bottle regulator iso valve) – OPEN, verify pressure at PG6
    Note: Verify pressure at PG6 on front of gas panel
    Note: All gas flow operations are now conducted from the front side of the gas panel using panel-mounted regulators and valves.

SYSTEM EVACUATON/VACUUM TESTING

1. H_2 burn off switch – ON
   Note: The igniter filament in the hood will glow red hot.

2. SV1 power switch – ON
   Note: SV1 will open within 10 seconds accompanied by a click sound.

3. V13 (vacuum pump exhaust) – OPEN

4. Vacuum roughing pump switch – ON

5. V11 (vacuum pump inlet) – OPEN

6. V10 (chamber exhaust valve) – OPEN
   Note: Evacuate system, leak check connections, and verify air leaving the pump.
   Note: Evacuate system until a vacuum of 30 mmHg (30 Torr) is established.
   Note: The vacuum system remains on throughout vacuum tests.
   Note: System lines are now evacuated up to MFC1 (H2 mass flow controller) and V9 (N2 control valve).
   Note: Evacuate until a vacuum of 29 inHg (25 Torr) as observed on PG9 (chamber pressure gauge) can be maintained.

7. Conduct vacuum SYSTEM HEAT-UP testing if desired by following next section, at conclusion, turn off RF heating before continuing to step 8 below

8. V11 – CLOSE

9. Vacuum pump – OFF

10. V13 - CLOSE

SYSTEM HEAT-UP

1. RF power supply breaker – ON

2. DAQ system – Start recording

3. Potentiometer – Set power input level to _____

4. RF power supply start button – PUSH ON
   Note: Verify heating by observing RF power supply heating indicator, monitoring pyrometer display and DAQ system
   Note: Verify sample heating by observing chamber sight glass.
   Note: Monitor chamber and cooling water temperatures.
   ***Caution*:** Furnace exterior maximum operating temperature is 150°C. If temperature exceeds set-point decrease potentiometer set-point or disrupt power.
   WARNING: Furnace and/or exhaust stack may be hot and could cause injury if touched.

5. Element at desired temperature – Reduce input power
   Note: Temperature will stabilize

GAS FLOW INITIATION

1. set PR3 (Ar panel regulator) to 10 psig
   Note: observe pressure setting of 10 psig on PG7

2. set PR4 (H_2 panel regulator) to 10 psig
   Note: observe pressure setting of 10 psig on PG8

3. V5 – OPEN

4. H_2 mass flow controller set point – _____ (16.5 SLPM (16500 SCCM) is typical for sample test)
   ***Caution*:** Never adjust the set-point to a non-zero value if no gas pressure is available to make flow as the valve will become very hot.
   Note: observe chamber filling with H2 from vacuum to 0 psig on PG9

5. When PG9 reads 0 psig, V12 – OPEN

6. Timer – START
   Note: confirm flow of H_2 by observing hydrogen gas flame at exhaust stack in fume hood
   Note: record start time _____

7. Allow for sample exposure to occur for _____ minutes then proceed with **SHUT DOWN** procedures.

SHUT DOWN

1. RF Power supply button – OFF
   Warning: Allow furnace to cool to 25 °C before removing samples.

2. V2 (H_2 bottle valve)– CLOSE

3. H_2 mass flow controller set point – 1.0 SLPM (1000 SCCM)

4. V6 – OPEN

5. V8 – OPEN

6. V9 – OPEN
   Note: Flow Ar through H_2 lines until burn-off stack no longer has a flame. SV1 should make an audible click as it closes

7. H_2 mass flow controller set point – 0.0 SLPM

8. V9 - CLOSE

9. V1 – CLOSE

10. V7 – OPEN
    Note: The Ar panel regulator gauge PG7 and H_2 panel regulator gauge PG8 should both read 0 psig.

11. V8 – CLOSE

12. V7 – CLOSE

13. V6 – CLOSE

14. V5 – CLOSE

15. PR3 – FULL CCW

16. PR4 – FULL CCW

17. V4 – CLOSE (BACK OFF H_2 BOTTLE REGULATOR, FULL CCW)

18. V3 – CLOSE (BACK OFF Ar BOTTLE REGULATOR, FULL CCW)

19. V10 – CLOSE

20. V12 – CLOSE

21. H_2 burn off switch – OFF
    ***Caution*:** The igniter will still be hot.

22. H_2 monitors – OFF

23. Portable oxygen detector - OFF

24. DAQ System Recording – STOP

25. 480 VAC power cord for RF power supply – UNPLUG

26. 208 VAC power for RF power supply chill water Recirculator – SWITCH OFF, UNPLUG

27. 110 VAC power cords for instrumentation and vacuum pumps – SWITCH OFF, UNPLUG
    Note: Vacuum pump will not have power available.

28. 110 VAC power cords for mass flow controllers and solenoid valve control system – SWITCH OFF,UNPLUG
    Note: H_2 gas flow controller display will no longer be active.
    Note: Hydrogen burn off system will not have power available.

29. 230 VAC power cord for RF coil and chamber cooling water Recirculator (located in 105 high bay outside of 4205/105E processing lab) – SWITCH OFF, UNPLUG

SAMPLE REMOVAL AND POST PROCESSING

1. Chamber top flange – Remove
2. Molybdenum thermal shield top - Remove
3. Insulator – Remove
4. Sample – Remove and place in a plastic bag
5. Sample pedestal – Clean with acetone

DOWN-STREAM MASS FLOW CONTROLLER RELIEF VALVE ACTIVATION

Note: Conduct this procedure if RV4 activates.

1. V9 – Check flow (CW turns) until reduced flow rate allows relief valves to reseat

2. H_2 mass flow controller – Decrease flow rate until relief valves reseat
   Note: If the relief valves do not reseat proceed with step 3.

3. V2 – Close

4. V1 – Close
   Note: If steps 3 and 4 are ineffective evacuate the laboratory and contact appropriate personnel.

UP-STREAM MASS FLOW CONTROLLER RELIEF VALVE ACTIVATION

Note: Conduct this procedure if RV1 or RV2 activate.

1. PR3 – Adjust Ar panel regulator CCW until relief valves reseat

2. PR4 – Adjust H_2 panel regulator CCW until relief valves reseat
   Note: If the relief valves do not reseat proceed with step 3.

3. V2 – CLOSE

4. V1 – CLOSE
   Note: If previous steps are ineffective evacuate the laboratory and contact appropriate personnel.

EMERGENCY SHUTDOWN

1. **V2 – CLOSE**
2. **V8 – OPEN**
3. **RF POWER SUPPLY SWITCH – OFF**
4. **V6 – OPEN**
5. **V9 – OPEN**

   Warning: If conditions permit, continue with the following steps. If not, evacuate laboratory and contact appropriate personnel.

6. Ar system purge of H_2 until burn-off stack flame extinguished
7. V9 – CLOSE
8. H_2 mass flow controller set point – 0.0 SLPM
9. V1 – CLOSE
10. V7 – OPEN
11. V12 – CLOSE
12. 480 VAC power cord for RF power supply – UNPLUG
13. 208 VAC power for RF power supply chill water Recirculator – SWITCH OFF, UNPLUG
14. 110 VAC power cords for instrumentation and vacuum pumps – SWITCH OFF, UNPLUG
    Note: Vacuum pump will not have power available.
15. 110 VAC power cords for mass flow controllers and solenoid valve control system – SWITCH OFF,UNPLUG
    Note: H_2 gas flow controller display will no longer be active.
    Note: Hydrogen burn off system will not have power available.
16. 230 VAC power cord for RF coil and chamber cooling water Recirculator (located in 105 high bay outside of 4205/105E processing lab) – SWITCH OFF, UNPLUG
17. Evacuate laboratory and contact appropriate personne

REFERENCES

1. Bruno, C. (ed.): *Nuclear Space Power and Propulsions Systems—Progress in Astronautics and Aeronautics*, AIAA, Vol. 225, 282 pp., Reston, VA, July 2008.

2. Emrich, W.J.: *Nuclear Thermal Rocket Element Environmental Simulator (NTREES)*, NASA 20080015668, Marshall Space Flight Center, Huntsville, AL, February 2008.

3. Felice, R.A.: *The Spectropyrometer—A Practical Multi-Wavelength Pyrometer*, Presentation, 8th Symposium on Temperature: Its Measurement and Control in Science and Industry, Chicago, IL, October 21–24, 2002.

4. Gupta, S.D.; Gupta, S.K.; and Jha, P.K.: "High Pressure Study on the Phonon Spectra and Thermal Properties in Hafnium Nitride and Zirconium Nitride," *J. Therm. Anal. Calorim.*, Vol. 107. No. 1, pp. 45–53, June 2011.

5. Meek, J.M.; and Craggs, J.D.: *Electrical Breakdown of Gases*, John Wiley & Sons, Ltd., New York, NY, pp. 878, 1978.

6. Arnold, A.H.M.: "The Alternating Current Resistance of Tubular Conductors," *J.I.E.E.,* Vol. 78, No. 473, pp. 580–593, May 1936; Discussion, *J.I.E.E.*, Vol. 79, pp. 595–596, March 1936.

7. Jet Propulsion Laboratory, California Institute of Technology, *Jupiter Icy Moons Orbiter (JIMO) an element of the Prometheus Program, Annual Report*, 982-R06933, JPL 04-016 10/04, Pasadena, CA, October 2004.

REPORT DOCUMENTATION PAGE

Form Approved
OMB No. 0704-0188

1. REPORT DATE *(DD-MM-YYYY)*	2. REPORT TYPE	3. DATES COVERED *(From - To)*
01–12–2012	Technical Memorandum	

4. TITLE AND SUBTITLE

Compact Fuel Element Environment Test

5a. CONTRACT NUMBER

5b. GRANT NUMBER

5c. PROGRAM ELEMENT NUMBER

6. AUTHOR(S)

D.E. Bradley,* O.R. Mireles, R.R. Hickman, and J.W. Broadway

5d. PROJECT NUMBER

5e. TASK NUMBER

5f. WORK UNIT NUMBER

7. PERFORMING ORGANIZATION NAME(S) AND ADDRESS(ES)

George C. Marshall Space Flight Center
Huntsville, AL 35812

8. PERFORMING ORGANIZATION REPORT NUMBER

M–1352

9. SPONSORING/MONITORING AGENCY NAME(S) AND ADDRESS(ES)

National Aeronautics and Space Administration
Washington, DC 20546–0001

10. SPONSORING/MONITOR'S ACRONYM(S)

NASA

11. SPONSORING/MONITORING REPORT NUMBER

NASA/TM—2012–217476

12. DISTRIBUTION/AVAILABILITY STATEMENT

Unclassified-Unlimited
Subject Category 20
Availability: NASA CASI (443–757–5802)

13. SUPPLEMENTARY NOTES

Prepared by the Propulsion Systems Department, Engineering Directorate
*Yetispace, Inc., Huntsville, AL

14. ABSTRACT

Deep space missions with large payloads require high specific impulse (I_{sp}) and relatively high thrust to achieve mission goals in reasonable time frames. Conventional, storable propellants produce average I_{sp}. Nuclear thermal rockets (NTRs) capable of high I_{sp} thrust have been proposed. NTR employs heat produced by fission reaction to heat and therefore accelerate hydrogen, which is then forced through a rocket nozzle providing thrust. Fuel element temperatures are very high (up to 3,000 K) and hydrogen is highly reactive with most materials at high temperatures. Data covering the effects of high-temperature hydrogen exposure on fuel elements are limited. The primary concern is the mechanical failure of fuel elements that employ high melting point metals, ceramics, or a combination (cermet) as a structural matrix into which the nuclear fuel is distributed. It is not necessary to include fissile material in test samples intended to explore high-temperature hydrogen exposure of the structural support matrices. A small-scale test bed designed to heat fuel element samples via noncontact radio frequency heating and expose samples to hydrogen for typical mission durations has been developed to assist in optimal material and manufacturing process selection without employing fissile material. This Technical Memorandum details the test bed design and results of testing conducted to date.

15. SUBJECT TERMS

NTP, nuclear thermal propulsion, NTR, nuclear thermal rocket, cermet, RF heating, nuclear fuel screening, pyrometry, hydrogen furnace

16. SECURITY CLASSIFICATION OF:			17. LIMITATION OF ABSTRACT	18. NUMBER OF PAGES	19a. NAME OF RESPONSIBLE PERSON
a. REPORT	b. ABSTRACT	c. THIS PAGE			STI Help Desk at email: help@sti.nasa.gov
U	U	U	UU	76	19b. TELEPHONE NUMBER *(Include area code)* STI Help Desk at: 443–757–5802

National Aeronautics and
Space Administration
IS20
George C. Marshall Space Flight Center
Huntsville, Alabama 35812